Lithos 153 (2012) 94–107

Contents lists available at SciVerse ScienceDirect

Lithos

journal homepage: www.elsevier.com/locate/lithos

# Early Variscan I-type pluton in the pre-Alpine basement of the Western Alps: The ca. 360 Ma Cogne diorite (NW-Italy)

François Guillot [a,*], Jean-Michel Bertrand [b,1], François Bussy [c], Pierre Lanari [d], Ludovic Cosma [c,2], Christian Pin [e]

[a] Université Lille Nord de France, CNRS – FRE 3298 Géosystèmes, UFR Sciences de la Terre, F-59655 villeneuve d'Ascq CEDEX, France
[b] 15 chemin d'Avat, F-38240 Meylan, France
[c] Institut de Minéralogie et de Géochimie, Université de Lausanne, Anthropole, CH-1015 Lausanne, Switzerland
[d] ISTerre, Université de Grenoble I, UMR CNRS/UJF 5275, 1381 rue de la Piscine, F-38041 Grenoble, France
[e] Département de Géologie, CNRS Université Blaise Pascal, 5 rue Kessler, F-63038 Clermont-Ferrand CEDEX, France

ARTICLE INFO

*Article history:*
Received 31 October 2011
Accepted 5 April 2012
Available online 16 April 2012

*Keywords:*
Early Variscan
Hornblendite
Sm–Nd isotopic ratios
Magmatic thermobarometry
Magmatic sources
Alpine nappe model

ABSTRACT

Located at the internal border of the Grand-Saint-Bernard Zone, the diorite and its aureole lie on top of intensively studied Alpine eclogitic units but this pluton, poorly studied yet, has kept locally almost undeformed. The pluton intruded, at ~360 Ma, country-rocks mostly composed of dark shales with $Na_2O > K_2O$ and minor mafic intercalations of tholeiitic basalt affinity. This association is characteristic of the Vanoise (France) basement series, where available age determinations suggest an Early Paleozoic age. Parts of the pluton, and of its hornfels aureole that is evidenced here for the first time, in the Punta Bioula section of Valsavaranche valley (NW-Italy), have been well-preserved from the Alpine deformation. Syn-emplacement hardening, dehydration-induced, probably prevented strain-enhanced Alpine recrystallization. Magmatic rock-types range continuously from subordinate mafic types at $SiO_2$ ~48%, of hornblendite with cumulative or appinite affinities, to the main body of quartz diorite to quartz monzonite ($SiO_2$ up to 62%). P–T estimates for the pluton emplacement, based on the abundance of garnet in the hornfelses, using also zircon and apatite saturation thermometry and Al-in-hornblende barometry, suggest T ~ 800–950 °C and minimum P in the 0.2–0.5 GPa range, with records of higher pressure conditions (up to 1–2 GPa?) in hornblendite phlogopite-cored amphibole. The high-K, Na > K, calc-alkaline geochemistry is in line with a destructive plate-margin setting. Based on major element data and radiogenic isotope signature ($\varepsilon Nd_{360\ Ma}$ from −1.2 to +0.9, $^{87}Sr/^{86}Sr_{360\ Ma}$ from 0.7054 to 0.7063), the parental magmas are interpreted in terms of deep-seated metabasaltic partial melts with limited contamination from shallower sources, the low radiogenic Nd-content excluding a major contribution from Vanoise tholeiites. There is no other preserved evidence for Variscan magmatism of similar age and composition in the Western Alps, but probable analogs are known in the western and northern parts of French Massif Central. Regarding the Alpine tectonics, not only the age of the pluton and its host-rocks (instead of the Permo-Carboniferous age previously believed), but also its upper mylonitic contact, suggest revisions of the Alpine nappe model. The Cogne diorite allegedly constituted the axial part of the E-verging "pli en retour [backfold] du Valsavaranche", a cornerstone of popular Alpine structural models: in fact, the alleged fold limbs, as attested here by field and geochemical data, do not belong to the same unit, and the backfold hypothesis is unfounded.



## 1. Introduction

Assessing the tectonic setting and P–T conditions of emplacement of granitoid bodies relies on a wide choice of methods. For fresh rocks, the study of mineral assemblages, mineral zoning and mineral chemistry may be privileged upon the consideration of "blind" whole-rock geochemical indicators. In case of secondarily metamorphosed plutons, this approach is not applicable any more, and it is necessary to use more indirect methods, based on immobile element contents at the whole rock scale, and refractory minerals. Here we attempt to characterize the Cogne diorite, a plutonic body that belongs to the polycyclic, pre-Triassic basement of the Western Alps, with special effort to separate the pre-Alpine heritage from the Alpine overprinting.

The Cogne diorite pluton crops out in the basement of the Middle Penninic Zone. Its igneous emplacement occurred near the Devonian–Carboniferous boundary, as documented by U–Pb zircon dating (Bertrand et al., 2000b) at ~360 Ma, so that this pluton is a rare, if not the only, piece of evidence of the early stage of the Variscan events in the Western Alps. Here we present new geochemical and petrological

* Corresponding author. Tel.: +33 320436731; fax: +33 320434910.
*E-mail address:* francois.guillot@univ-lille1.fr (F. Guillot).
[1] Deceased, March 18th, 2011.
[2] Present address: 8bis route d'Avignon, F-13410 Lambesc, France.

0024-4937/$ – see front matter © 2012 Elsevier B.V. All rights reserved.
doi:10.1016/j.lithos.2012.04.010

data for the Cogne diorite as an opportunity to assess the Early Carboniferous, or older, tectonic setting of yet poorly known pre-Alpine domains. In a context of Alpine high pressure and subduction-related nappes, tracing the origin of the units requires to take into account their protolith ages. A number of protolith age determinations have been obtained during the last decades on such pre-Alpine basement units, often with unexpected results, leading to various paleogeographic inferences (Bertrand et al., 2005; Michard and Goffé, 2005; Ring et al., 2005). It seems timely to unravel the pre-Alpine geological history of some of those recently dated units.

## 2. Geological context

Many unresolved questions arise from the location of the Cogne pluton in the internal zone of the Alpine orogen (Figs. 1–3, Table 1), inserted in a complex nappe stack. Regarding the Alpine events, P–T-t estimates of 1.5–3 GPa, 575 °C at 45–30 Ma have been published for the Gran Paradiso basement massif (Gabudianu Radulescu et al., 2009) and its Alpine cover (Angiboust et al., 2009; Beltrando et al., 2009). The determination of these eclogitic conditions is critical, because these units, corresponding to the most deeply subducted

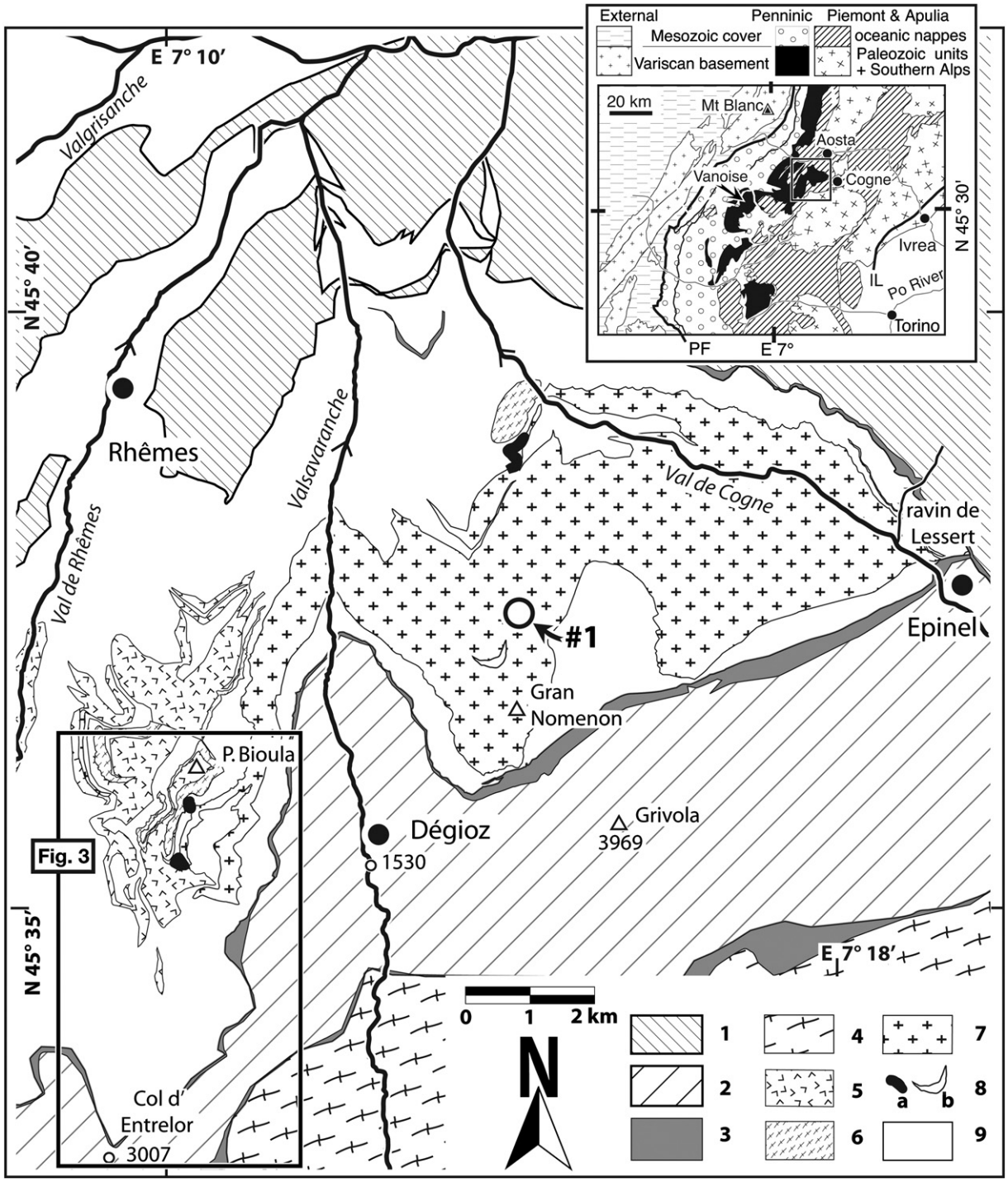


**Fig. 1.** Geological map of the Cogne diorite. Key to symbols and abbreviations. *Inset* — PF, Penninic Front — IL, Insubric Line. *Main frame* — #1, location of sample 1 — *Key to formations.* — 1, Combin calcschists with minor ophiolite — 2, eclogitic Zermatt-Saas Fee calcschists and major eclogitized metaophiolite — 3, evaporite-rich and often brecciated, carbonated rocks of presumed Triassic age — 4, eclogitized Gran Paradiso Permian orthogneiss — 5, Punta Bioula summit gneiss minuti — 6, Punta Bioula summit augengneiss — 7, Cogne diorite — 8a, appinite pods — 8b, leucogranite — 9, carbonaceous host rocks — P. Bioula, Punta Bioula.

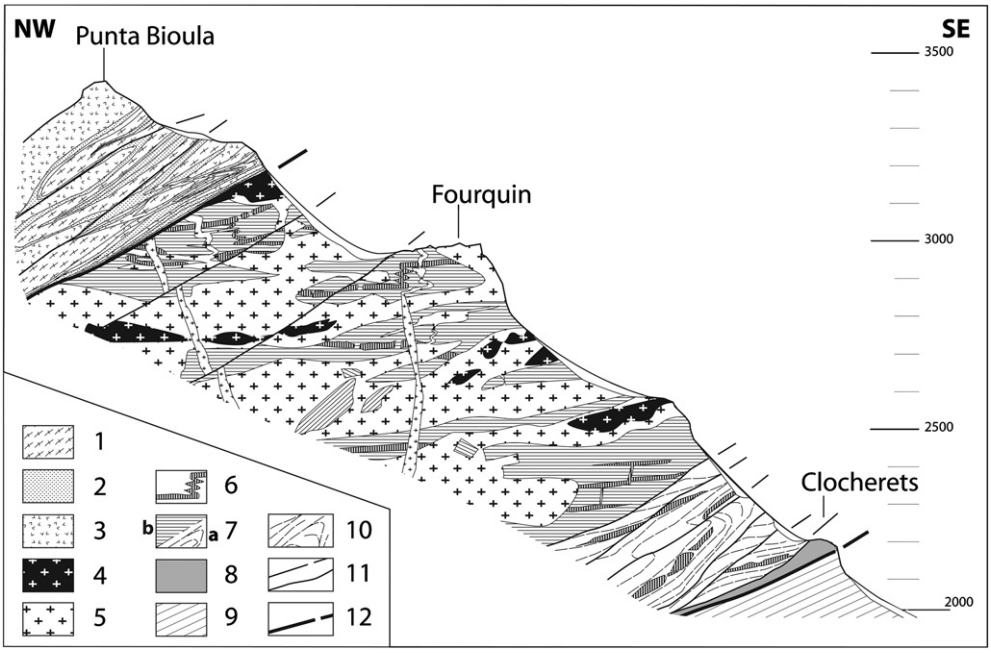


**Fig. 2.** Interpretative sketch of the Punta Bioula section. 1–3, TPBU formations (resp. augengneiss, quartz-mylonite, gneiss minuti) — 4–10, Cogne diorite unit formations: 4, hornblendite — 5, diorite — 6, host rock mafic sills and dykes — 7a, host rock metapelites, 7b, hornfelses and migmatites — 8, carbonated breccia, presumably from a Triassic dolomite protolith — 9, calcschists with eclogitized ophiolite (Jurassic) — 10–12, Alpine foliation and faults (Tertiary).

Alpine units, lie right under the diorite-hosting basement unit. Based on the presence of garnet- and glaucophane-white mica assemblages in some diorite samples and of jadeite pseudomorphs in augengneiss (Cigolini, 1995) of the Top Punta Bioula Unit (TPBU, as defined in Section 2.2.2), Bucher and Bousquet (2007) have concluded that the Cogne pluton suffered a high-P event. Discussing either the Alpine vs. pre-Alpine age of mineral assemblages, or the peak Alpine conditions, is out of the scope of this paper. A provisional pseudosection, based on analysis #9 and garnet–actinolite–phengite–clinozoisite–quartz mineral chemistry of the same rock, yields $1.7 \pm 0.2$ GPa with $540 \pm 50$ °C (work in progress). This strongly recrystallized mafic diorite was sampled a couple of meters under the top of the diorite-hosting unit. There, our field data (Section 2.2.2) provide evidence for a first order tectonic contact separating the diorite-hosting unit, almost free of Alpine deformation, from the heavily deformed overlying TPBU, and we further document (Section 3) geochemical differences between those units.

### 2.1. Milestone works on the Cogne diorite

Novarese (1894, 1909) defined the pluton as a quartz diorite, inferring its intrusive nature from apophyses and nodular schists. Based on their graphite content and black color, the host rocks were interpreted as Carboniferous meta-sediments and a Permo-Carboniferous age was proposed for the intrusion (Novarese, 1909: p. 511). Followed by many other authors, Argand (1910, 1911) admitted those ages, a stratigraphic tenet which partly founded his seminal tectonic interpretation of the Alps as a nappe pile. The Cogne diorite was supposed to be at the heart of a key Alpine anticline of nappes, the "Valsavaranche backfold". The Cogne region was also the place where Amstutz, while again defending a Permo-Carboniferous age, coined the notion of subduction (in 1949, after White et al., 1970) in order to explain the outward dip of the nappe stack, to the NW, as an alternative to Argand's backthrust model. A petrographical study of the Cogne diorite and of its aureole was performed by Grasso (1974), by means of optical microscopy only. He described relict pre-Alpine feldspars, largely replaced by burgeoning albite. He also proposed criteria for separating ancient minerals (biotite, garnet, amphibole) from Alpine re-crystallized ones, reporting a biotite ghost inside an amphibole phenocryst, and one inferred andalusite crystal replaced by sericite.

### 2.2. Field data

#### 2.2.1. Main units

The pluton and its aureole, the latter being tentatively contoured for the first time in the present paper, have not yet been subjected to a systematic mapping of their various rock types, except by Amstutz (1962) to the E of the Valsavaranche valley. Here we focus on the W side of the Valsavaranche where most of our rocks were sampled, in the Punta Bioula massif (Fig. 1). As a summary of our field work, a tentative section has been drawn along the trail that leads from Valsavaranche up to the top of the Punta Bioula (Fig. 2), together with a provisional, local map of the high crest joining Punta Bioula to Col d'Entrelor (Fig. 3).

At its footwall, the diorite-hosting unit rests upon a thin veneer of Triassic-looking limestone lenses, also named Entrelor Shear Zone. Both tectonically overlie oceanic Piemont units with their calcschist cover (Jurassic to Tertiary in age) imbricated with ophiolite basement slivers (dated elsewhere in the Western Alps around 155–165 Ma). The Entrelor Shear Zone is interpreted as a major low-angle fault, although its reverse (backthrust) or normal (exhumation) kinematics remains controversial. This debate is related to the model of "Valsavaranche backfold", subject of a well-documented discussion by Bousquet (2008, his Fig. 3, and references therein). From the field data exposed hereafter, another major low-angle fault is probably also present at the hanging wall of the diorite-hosting unit.

#### 2.2.2. TPBU unit

At its top, the diorite-hosting unit is capped directly by a rock unit, that we call TPBU, devoid of diorite. Here, along the Punta Bioula-Col d'Entrelor crest line, Cigolini (1992, 1995) has mapped in detail various formations (reddish quartzite and white quartzite bands, augengneiss, albitic gneiss, prasinitic gneiss) constituting the Punta Bioula above 3100 m (Figs. 1–3). Cigolini further proposed an Upper Permian age for this unit, interpreted to represent an unconformable cover for the diorite. Following Caby (1968) and Hermann (1925), he also mentioned the prominent, km-sized recumbent folds outlined by the TPBU

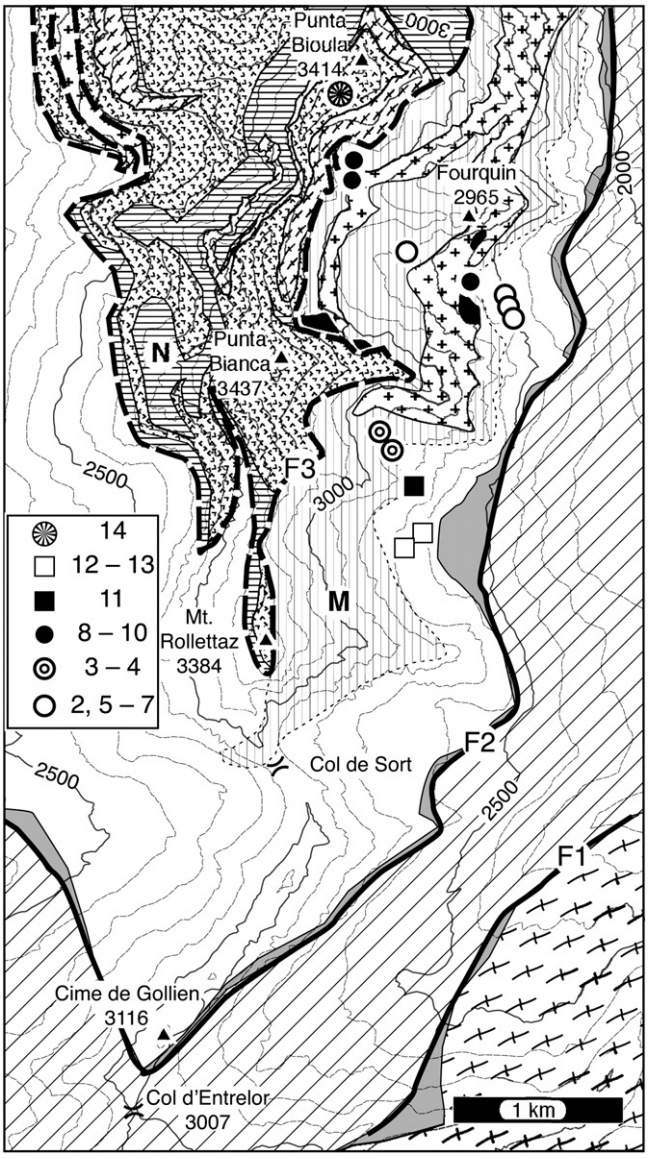


**Fig. 3.** Geological map of the Punta Bioula area (after Cigolini, 1992, and new field work). Key to formations as in Fig. 1, except: M (vertical cross-hatching), quartz-veined hornfelses and migmatized country-rock related to the diorite pluton intrusion; N, undetermined rocks from the TPBU (analog of 7a in Fig. 2, after Cigolini, 1992). Main tectonic contacts: F1, low-angle fault separating oceanic, Jurassic calcshists and ophiolite of the Col d'Entrelor from Gran Paradiso orthogneiss — F2, low-angle fault between oceanic unit and Middle Penninic basement — F3, presumed tectonic contact of the TPBU over the Cogne diorite-hosting unit.

**Table 1**
Main rock types, classified by their presumed age, in the Punta Bioula section (Fig. 2). Explanations in text.

| Age/rock type | Mafic formations | Felsic formations | Sediments, volcanics |
|---|---|---|---|
| 356–360 Ma calc-alkaline pluton | Hornblendite (appinite?) anal. 8 to 10 | Quartz diorite to granodiorite anal. 1 to 7 | Unknown |
| Unknown age, TPBU | Prasinite | Augengneiss, quartzite | Gneiss minuti, anal. 14 |
| 510–480 Ma A-type, bimodal rocks, and associated dark metapelite | Tholeiite levels anal. 11 + anal. in litt. | Granophyre felsic metavolcanites anal. in litt. | Metapelite and metagreywacke series anal. 12–13 + in litt. |

reddish quartzite levels. We concur with Cigolini that the TPBU does not contain any diorite body and appears to be in sharp contact with the diorite and its aureole. However a dilemma arises from his age assumptions, not only because no dating has yet been performed of the supposedly Upper Permian formations, but also because the intense deformation rather suggests a tectonic emplacement over the diorite-hosting unit, a hypothesis supported by our field observations near the contact.

The lowermost outcrop at the footwall of the TPBU is an ~10 m thick quartzite layer (Fig. 4) outcropping at 3180 m a.s.l. between Fourquin and Punta Bioula (Fig. 2). The rock is made of sub parallel, mm- to cm-thick quartz-ribbons separated by feldspar- and phengite-rich, scaly-looking bands (Fig. 4a) that resemble the overlying augengneiss. Actually, transitional terms are observable: e.g., following this formation to the NE, the quartzite layer gets thicker (~30 m) around 3220 m a.s.l., with a flat-lying, crude layering affected by isoclinal, mm- to m-scale, W-verging folds (Fig. 4b), comprising folded augengneiss lenses. The intimate association with augengneiss and their isoclinal folding are suggestive of a mylonitic zone, with a top-

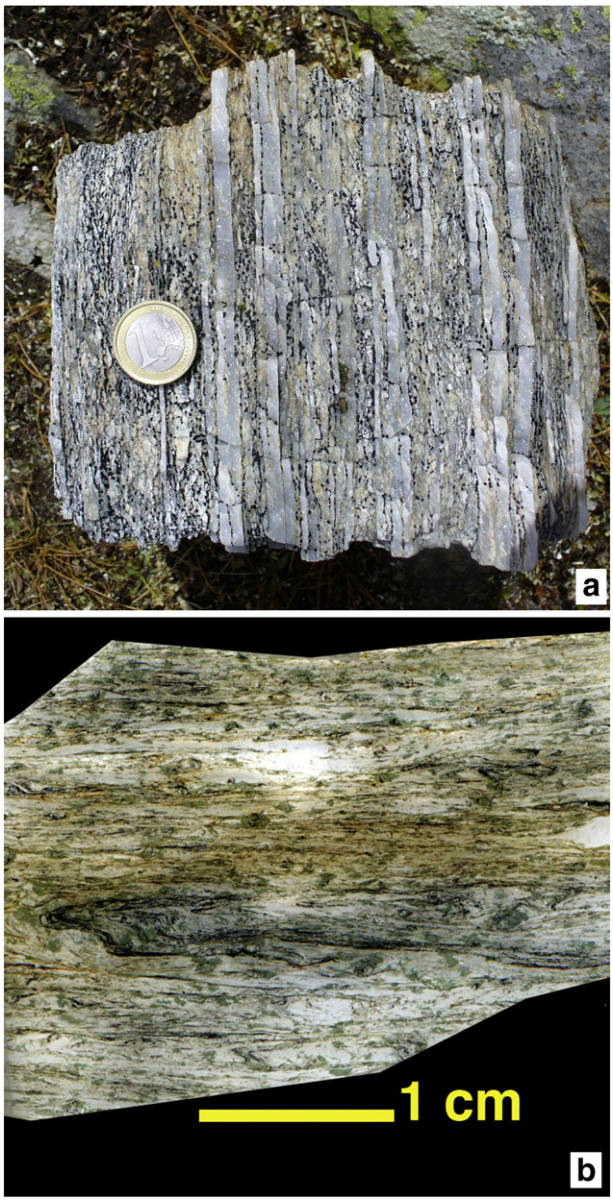


**Fig. 4.** Mylonites at the footwall of the TPBU. a, Mylonite of alternating bluish quartzite lens and micaschist–augengneiss layers — b, tight folds in mylonitic micaschist (scanned thin section, sample G03101). Location, 3170 m a.s.l., Punta Bioula trail.

to-the-W sense of shear, rather than of a metasedimentary sequence. Taking also into account the tight recumbent folds that affect the TPBU formations, the diorite and its aureole (M in Fig. 3) are interpreted as in tectonic contact with the TPBU, along an Alpine thrust plane (F3 in Fig. 3) gently dipping W to NW (parallel, top-to-the-W, minor shear zones have also been observed across the diorite-hosting unit near the Fourquin, that were suggestively sketched in Fig. 2). This provisional interpretation departs from the traditional view of a two-limbed anticline, with the Cogne diorite in its hinge (the "Valsavaranche backfold"), and needs to be checked by further works. Hereafter it is shown that the geochemical characters of the diorite and its host-rocks present distinct differences with the TPBU.

*2.2.3. Diorite and aureole outcrops*

The diorite-hosting unit has a basal part near the Clocherets (Fig. 2, 2200 to 2450 m a.s.l.) of metapelites with dismembered greenstone levels, heavily deformed (Fig. 5a), as it is usual in Vanoise. In those banded, black, gray or greenish metapelites, no obvious

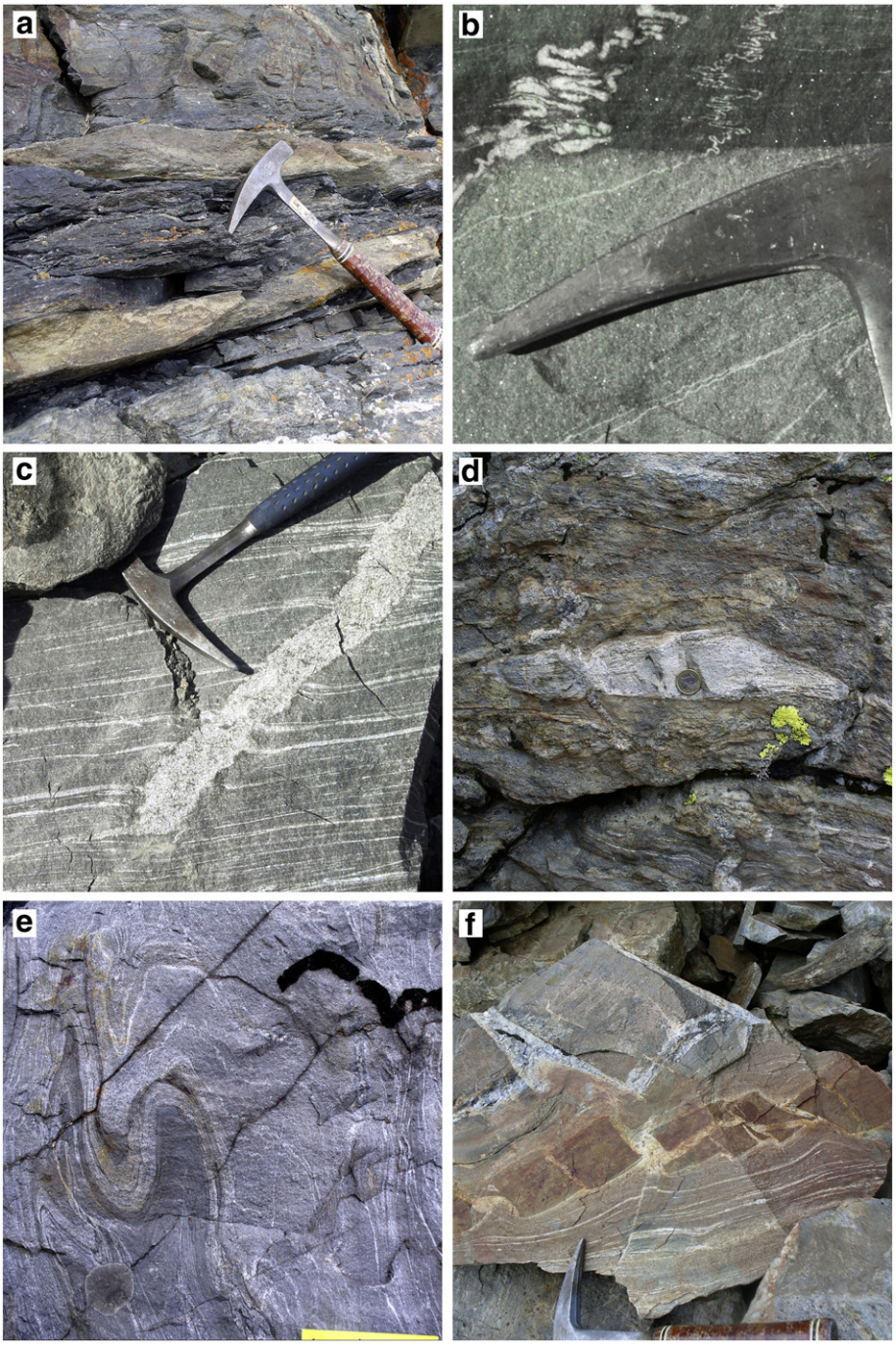


**Fig. 5.** Host-rocks. a, Distal relative to the diorite, Vanoise-type banded metapelite, with sub-horizontal Alpine cleavage — b, ptygmatically folded quartz veins across a lithological boundary between light, quartzitic level and a dark, carbonaceous level, revealing a much stronger deformation of the latter — c, melt-fed vein cross-cutting a sub-parallel net of early quartz veins — d, proximal [to a diorite body] melt-fed, lozenge-shaped wedge — e, proximal, contorted folds, — f, proximal, fragile boudinage of a reddish, mafic refractory level enclosed in veined metapelites, with leucocratic inter-boudin melt, and [bluish] late quartz-pegmatite veins at the top. Scales: hammer in a, b, c, f; 1-euro coin in d; 12-cm yellow paper sticker in e. No Alpine deformation is observable, except in a. Locations (names as in Fig. 3) — a, 2500 m, base of Punta Bianca eastern cliff — b, 2700 m, 1 km NE from Mt. Rollettaz — c, moraine at 2500–2800 m along the Punta Bioula trail — d and f, Fourquin, 2950 m — e, 2825 m, NE slope of Punta Bianca.

bedding polarity was ever ascertained (except a rather loose mention of cross-bedding by Debelmas et al., 1991 without localization). By contrast over 2450 m a.s.l., hornfelses, migmatites and magmatic rocks prevail, that suffered much less intense Alpine deformation. Whether the greenstone levels of the country-rock represent lava flows, or later intrusions as sills, could not be ascertained elsewhere in Vanoise because of the stronger Alpine overprint. Here, branched networks of dark green bands observed in the proximal aureole near the Fourquin, a possible sill-and-dike system (Fig. 2), suggest an intrusive emplacement.

Near the Fourquin summit (Fig. 2), a number of well-preserved granitic rock types occur between 2450 and 3170 m a.s.l., complexly interleaved with strongly migmatized host-rocks (Figs. 5c–e, 6) characterized by a rusty weathering (Fig. 5d,f) and a dense veining. These rocks are all suggestive of a relatively high degree of partial melting: garnet-rich leucocratic lenses (Fig. 5d); zoned granitic veins (Figs. 5c, 6c); diorite pods with sub-orbicular texture, pegmatite veins and pockets (Fig. 5f); various transitions between felsic and mafic varieties (Fig. 6a); syn-magmatic deformation of the migmatized host-rock (Fig. 5e,f). Details about the hornblendites, that we only observed as drift, are given along with their geochemical description (see Fig. 6 a–b, and Section 3.4.1).

To the south of those proximal facies, more distal hornfelses have been observed, especially on the eastern slopes of Mt. Rollettaz and Punta Bianca (M in Fig. 3). The rocks are massive, fine-grained, very hard, and do not show any Alpine foliation, a major difference with the common Vanoise metapelites (Fig. 5a). A preserved layering made of alternating, cm to m-thick, black and gray bands, is crossed at all angles by a network of white quartz veins with intricate ptygmatic folding (Fig. 5b). A primitively high kerogen-content of the black layers is suggested by a study of the ptygmatic veining (Guillot, 2011) and differential flattening between gray and black layers (Fig. 5b). Hence, the emplacement of the diorite might have happened under C-rich, fluid-saturated conditions.

### 2.3. Age of the pluton and of its host-rocks

The Penninic basement units, though dominant in volume relative to the cover units of Meso-Cainozoic age, were poorly known until the late nineties. Traditional views favored a Permo-Carboniferous age emplacement for the Cogne diorite, merely based on the black color of its host-rocks believed to reflect a Late Carboniferous age. However, Bertrand et al. (2000b) measured a $363 \pm 24$ Ma ($2\sigma$) U–Pb zircon upper intercept age by ID-TIMS on a light-colored granodiorite, and a more precise $357 \pm 6$ Ma ($2\sigma$) age by SHRIMP on a darker sample, richer in amphibole, both samples taken near Epinel (loc. Fig. 1).

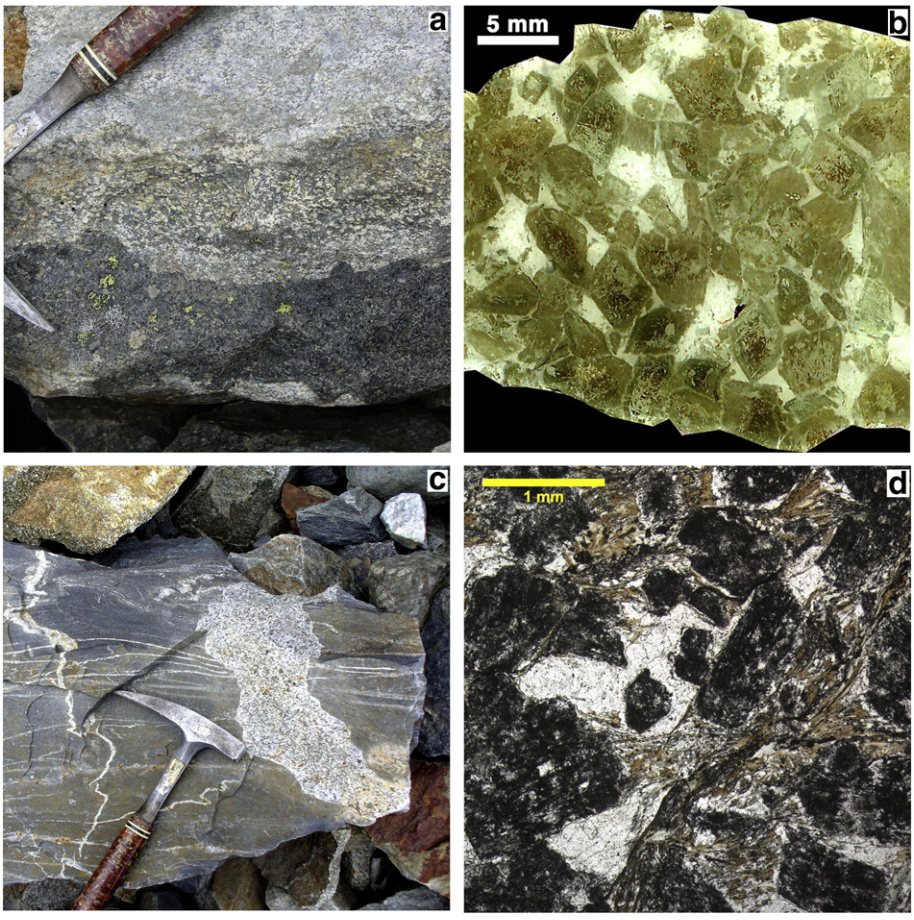


**Fig. 6.** Cogne diorite rock types. a, Horblendite horizon (bottom, under the hammer pick) with lobate contact with (at middle height) porphyritic diorite (anal. 2, 6, 7 in Table 2), succeeded (top) by a leucocratic rock type — b, horblendite (anal. 8 in Table 2) thin section (scanned image, enhanced colors), with white xenomorphic feldspar and quartz, green euhedral hornblende crystals often containing a biotite core and/or brown hornblende (dark red dyes); — c, dm-thick plagiodiorite vein, in host-rock metapelite crossed by a net of ptygmatic quartz veins — d, plagiodiorite (anal. 5 in Table 2) thin section with euhedral, cloudy plagioclase (dark), xenomorphic, clear quartz (white), biotite (brown) (see also SM2, image 5). Note the absence (in b) or weakness (in d) of post-magmatic deformation. — Location: moraine at 2500–2800 m along the Punta Bioula trail.

**Table 2**
Analyzed samples. ROCK-TYPES (thin section images given as electronic supplementary data SM2, mineral assemblages as Table SM3): 1, granodiorite — 2, porphyritic diorite — 3–4, deformed granodiorite — 5, plagiodiorite — 6, 7, porphyritic diorite — 8–10, hornblendite — 11, mafic layer in the host-rock series — 12, black host-rock metapelite — 13, pale gray host-rock metapelite — 14, TPBU albitic gneiss. — present. CHEMICAL DATA: <L.D., lower than detection level. T.sat.Ap, Apatite saturation temperature (Harrison and Watson, 1984). T.sat.Zr, zircon saturation temperature (Watson and Harrison, 1983).

| Analysis | 1 | 2 | 3 | 4 | 5 | 6 | 7 | 8 | 9 | 10 | 11 | 12 | 13 | 14 |
|---|---|---|---|---|---|---|---|---|---|---|---|---|---|---|
| Field sample | BK048 | G03069 | G03051 | G03054 | BK031 | BK006 | G03070 | BK009 | G03099 | G03103 | G03058 | BK034 | BK033 | BK018 |
| *Major elements (wt.%)* | | | | | | | | | | | | | | |
| $SiO_2$ | 62.25 | 58.56 | 61.59 | 61.36 | 55.26 | 53.44 | 52.96 | 50.96 | 50.51 | 48.12 | 50.90 | 59.14 | 64.13 | 72.16 |
| $Al_2O_3$ | 16.00 | 17.44 | 18.60 | 18.55 | 21.00 | 15.83 | 14.39 | 8.70 | 12.82 | 10.58 | 15.71 | 17.68 | 16.60 | 13.98 |
| $Fe_2O_3$ | 4.50 | 5.79 | 3.80 | 4.24 | 5.63 | 7.90 | 8.93 | 7.94 | 10.74 | 9.05 | 9.34 | 8.01 | 5.52 | 2.64 |
| MnO | 0.09 | 0.10 | 0.06 | 0.07 | 0.08 | 0.13 | 0.14 | 0.15 | 0.20 | 0.14 | 0.13 | 0.16 | 0.08 | 0.05 |
| MgO | 2.79 | 2.78 | 1.68 | 1.68 | 2.06 | 6.55 | 5.83 | 14.15 | 8.40 | 10.42 | 8.06 | 3.67 | 2.34 | 0.23 |
| CaO | 4.08 | 5.37 | 4.51 | 4.16 | 5.16 | 7.15 | 7.29 | 11.06 | 8.47 | 10.53 | 8.09 | 1.85 | 2.98 | 1.18 |
| $Na_2O$ | 3.76 | 4.05 | 4.37 | 4.73 | 4.99 | 3.23 | 4.25 | 1.73 | 2.71 | 2.07 | 3.68 | 3.60 | 4.67 | 4.55 |
| $K_2O$ | 3.22 | 2.33 | 2.55 | 2.67 | 2.48 | 2.26 | 1.72 | 1.16 | 1.67 | 2.69 | 1.14 | 2.41 | 1.21 | 3.52 |
| $TiO_2$ | 0.61 | 0.84 | 0.78 | 0.69 | 0.81 | 1.40 | 1.21 | 0.69 | 1.78 | 2.00 | 0.87 | 0.90 | 0.73 | 0.23 |
| $P_2O_5$ | 0.25 | 0.30 | 0.32 | 0.32 | 0.44 | 0.53 | 0.92 | 0.46 | 1.02 | 2.78 | 0.08 | 0.18 | 0.16 | 0.06 |
| LOI | 1.24 | 1.55 | 1.64 | 1.51 | 1.50 | 1.88 | 1.30 | 2.23 | 2.25 | 1.88 | 2.12 | 2.30 | 1.51 | 1.22 |
| Total | 98.77 | 99.10 | 99.89 | 99.98 | 99.40 | 100.29 | 98.93 | 99.23 | 100.54 | 100.25 | 100.12 | 99.90 | 99.94 | 99.80 |
| A/CNK | 0.94 | 0.92 | 1.02 | 1.02 | 1.04 | 0.76 | 0.65 | 0.36 | 0.59 | 0.42 | 0.71 | 1.49 | 1.15 | 1.04 |
| mg# | 55 | 49 | 47 | 44 | 42 | 62 | 56 | 78 | 61 | 70 | 63 | 48 | 46 | 14 |
| *Trace-elements (ppm)* | | | | | | | | | | | | | | |
| Ba | 1168 | 1194 | 1044 | 1703 | 1701 | 1087 | 834.3 | 833.9 | 616.5 | 1906 | 201.3 | 638.6 | 437.7 | 638.2 |
| Sr | 580.6 | 771.8 | 862.2 | 875.5 | 1052 | 527.2 | 457.1 | 231.8 | 319.3 | 274.8 | 228.4 | 175.7 | 388.4 | 44.95 |
| V | 75.63 | 112.6 | 59.6 | 54.97 | 68.07 | 212.3 | 214.4 | 158.3 | 373.9 | 208.7 | 123.2 | 111.3 | 91.87 | 3.174 |
| Zn | 64.22 | 77.74 | 49.36 | 85.45 | 91.27 | 98.04 | 101.8 | 75.36 | 129.6 | 129.1 | 106 | 116.8 | 65.52 | 60.97 |
| Zr | 156.8 | 193.8 | 421.3 | 379.8 | 381.6 | 232.7 | 225.9 | 144.5 | 117.1 | 119 | 59.79 | 154.4 | 210.5 | 306.8 |
| Rb | 107.7 | 77.49 | 81.39 | 89.47 | 85.67 | 75.54 | 57.6 | 21.73 | 54.85 | 90.62 | 38.61 | 71.05 | 39.66 | 93.08 |
| Y | 15.48 | 19.91 | 9.245 | 17.05 | 14.61 | 33.63 | 38.38 | 15.98 | 47.33 | 43.61 | 16.61 | 25.87 | 19.99 | 68.54 |
| Cr | 76.73 | 13.43 | 14.6 | 15.7 | 16.91 | 192.6 | 91.38 | 1196 | 65.29 | 39.2 | 201.9 | 80.71 | 73.53 | <L.D. |
| Cu | 6.871 | 4.707 | 3.487 | 11.9 | 8.579 | 18.01 | 39.57 | 24.28 | 20.65 | 35.71 | 6.685 | <L.D. | 6.665 | 8.298 |
| Co | 10.68 | 12.49 | 5.764 | 6.719 | 5.729 | 27.13 | 27.48 | 40.59 | 35.76 | 29.3 | 38.12 | 21.11 | 13.2 | 1.346 |
| Nb | 7.037 | 11.58 | 6.858 | 10.05 | 10.03 | 10.07 | 12.77 | 9.316 | 14.05 | 21.96 | 1.48 | 11.3 | 9.842 | 10.07 |
| Ga | 19.51 | 21.71 | 21.73 | 22.82 | 24.39 | 22.13 | 21.57 | 11.7 | 21.41 | 19.36 | 15.84 | 22.9 | 19.3 | 22.75 |
| Pb | 32.75 | 27.95 | 34.25 | 37.04 | 35.31 | 25.19 | 23.74 | 7.52 | 13.90 | 19.10 | 7.73 | 6.01 | 7.22 | 3.46 |
| Th | 27.41 | 13.55 | 8.301 | 23.53 | 26.39 | 6.249 | 10.72 | 5.227 | 9.759 | 16.45 | 0.616 | 7.978 | 7.153 | 11.67 |
| U | 7.474 | 6.457 | 5.838 | 8.028 | 7.14 | 5.335 | 6.694 | 2.616 | 7.442 | 8.597 | 0.278 | 2.002 | 1.486 | 3.468 |
| Ni | 23.68 | 6.328 | 5.802 | 7.163 | 6.041 | 73.6 | 29.12 | 128.1 | 13.81 | 6.894 | 69.39 | 48 | 33.43 | <L.D. |
| Hf | 4.503 | 5.251 | 10.11 | 9.566 | 9.942 | 6.235 | 7.279 | 4.156 | 4.346 | 4.501 | 1.581 | 4.499 | 5.643 | 8.705 |
| Sn | 2.561 | 2.818 | 0.685 | 1.518 | 1.876 | 2.698 | 6.206 | 3.093 | 7.636 | 3.983 | 1.528 | 2.061 | 1.216 | 4.167 |
| Cs | 4.968 | 3.233 | 3.136 | 4.202 | 3.706 | 3.286 | 3.78 | 0.745 | 1.528 | 3.817 | 1.415 | 2.049 | 1.72 | 1.28 |
| As | 3.145 | 5.824 | 3.431 | 2.678 | 1.735 | 2.098 | 6.164 | 2.59 | 7.849 | 3.371 | <L.D. | 3.945 | 1.425 | <L.D. |
| Be | 3.146 | 3.519 | 3.198 | 3.788 | 3.521 | 3.195 | 3.972 | 2.143 | 3.932 | 3.118 | 0.88 | 1.693 | 1.8 | 2.911 |
| Ge | 1.425 | 1.306 | 0.997 | 1.106 | 1.064 | 1.489 | 1.551 | 1.718 | 1.942 | 1.957 | 1.535 | 1.478 | 1.244 | 1.534 |
| Ta | 0.614 | 0.755 | 0.244 | 0.697 | 0.52 | 0.456 | 0.939 | 0.634 | 0.824 | 1.869 | 0.129 | 0.92 | 0.8 | 0.933 |
| Mo | <L.D. | <L.D. | 1.861 | <L.D. | <L.D. | <L.D. | <L.D. | <L.D. | 0.525 | 0.814 | <L.D. | <L.D. | <L.D. | <L.D. |
| W | 0.74 | 0.36 | 1.497 | 0.257 | 0.243 | 0.222 | 0.263 | 0.512 | 1.084 | 0.785 | 0.907 | 1.182 | 0.686 | 1.45 |
| Sb | 0.784 | 0.782 | 0.749 | 0.286 | 0.345 | 0.393 | 0.323 | 0.458 | 0.593 | 0.451 | 0.41 | 0.235 | 0.262 | 0.105 |
| Bi | <L.D. | <L.D. | <L.D. | <L.D. | <L.D. | <L.D. | <L.D. | <L.D. | <L.D. | 0.217 | 0.35 | <L.D. | <L.D. | <L.D. |
| In | <L.D. | 0.075 | <L.D. | <L.D. | <L.D. | 0.104 | 0.113 | 0.062 | 0.142 | 0.06 | 0.067 | 0.096 | <L.D. | 0.095 |
| Cd | <L.D. | <L.D. | <L.D. | <L.D. | <L.D. | <L.D. | <L.D. | <L.D. | <L.D. | <L.D. | <L.D. | <L.D. | <L.D. | <L.D. |
| T.sat.Ap (°C) | 921 | 899 | 943 | 940 | 905 | 905 | 987 | 846 | 966 | 1142 | 643 | | | 870 |
| T.sat.Zr (°C) | 755 | 762 | 853 | 841 | 829 | 732 | 701 | 533 | 630 | 544 | 619 | | | 845 |
| *REE (ppm)* | | | | | | | | | | | | | | |
| La | 47.84 | 31.56 | 17.15 | 54.47 | 62.92 | 27.33 | 34.21 | 24.06 | 47.79 | 88.44 | 3.568 | 26.62 | 29.76 | 40.32 |
| Ce | 92.57 | 62.12 | 29.94 | 98.05 | 116.3 | 66.11 | 92.27 | 55.58 | 125.8 | 204.1 | 8.84 | 55.61 | 58.64 | 86.37 |
| Pr | 9.862 | 7.369 | 3.292 | 10.5 | 12.43 | 8.863 | 13.46 | 7.098 | 16.8 | 26.47 | 1.322 | 6.727 | 6.868 | 10.72 |
| Nd | 33.57 | 28.31 | 12.18 | 35.98 | 43.27 | 38.94 | 59 | 28.67 | 67.81 | 110.6 | 6.572 | 26.18 | 26.11 | 42.85 |
| Sm | 5.267 | 5.505 | 2.223 | 5.797 | 6.648 | 8.927 | 12.59 | 5.769 | 13.34 | 21.24 | 2.057 | 5.644 | 4.991 | 10.03 |
| Eu | 1.186 | 1.517 | 1.253 | 1.559 | 1.757 | 1.987 | 2.832 | 1.424 | 2.791 | 4.651 | 0.868 | 1.327 | 1.278 | 1.372 |
| Gd | 3.715 | 4.391 | 1.896 | 4.116 | 4.38 | 7.967 | 9.795 | 4.371 | 10.66 | 14.91 | 2.565 | 5.12 | 4.279 | 10.2 |
| Tb | 0.519 | 0.629 | 0.259 | 0.562 | 0.564 | 1.132 | 1.356 | 0.599 | 1.522 | 1.853 | 0.439 | 0.788 | 0.64 | 1.762 |
| Dy | 2.841 | 3.595 | 1.494 | 3.048 | 2.812 | 6.337 | 7.445 | 3.173 | 8.533 | 9.117 | 2.831 | 4.812 | 3.754 | 11.12 |
| Ho | 0.529 | 0.685 | 0.308 | 0.576 | 0.507 | 1.162 | 1.354 | 0.552 | 1.567 | 1.511 | 0.595 | 0.936 | 0.726 | 2.304 |
| Er | 1.476 | 1.93 | 0.936 | 1.654 | 1.485 | 3.133 | 3.638 | 1.491 | 4.325 | 3.911 | 1.709 | 2.713 | 2.083 | 6.826 |
| Tm | 0.22 | 0.293 | 0.155 | 0.26 | 0.228 | 0.449 | 0.518 | 0.213 | 0.607 | 0.525 | 0.253 | 0.412 | 0.317 | 1.068 |
| Yb | 1.525 | 2.033 | 1.168 | 1.856 | 1.673 | 2.913 | 3.356 | 1.399 | 4.054 | 3.343 | 1.701 | 2.829 | 2.147 | 7.272 |
| Lu | 0.236 | 0.318 | 0.212 | 0.312 | 0.284 | 0.438 | 0.516 | 0.209 | 0.616 | 0.495 | 0.271 | 0.434 | 0.33 | 1.088 |
| $\sum$ REE | 201 | 150 | 72 | 219 | 255 | 176 | 242 | 135 | 306 | 491 | 34 | 140 | 142 | 233 |
| $La_N/Lu_N$ | 21.7 | 10.6 | 8.7 | 18.7 | 23.7 | 6.7 | 7.1 | 12.3 | 8.3 | 19.1 | 1.4 | 6.6 | 9.7 | 4.0 |
| $(Eu/Eu^*)_N$ | 0.82 | 0.94 | 1.87 | 0.98 | 1.00 | 0.72 | 0.78 | 0.87 | 0.72 | 0.80 | 1.16 | 0.75 | 0.85 | 0.41 |

This result implies a pre-Carboniferous age for the host rocks. Due to the lack of fossils and to the scarcity of detrital zircon, the age of this dark metapelite series, and of its m-thick intercalations of tholeiitic greenstone, has not yet been better constrained but is certainly older than the ~360 Ma intrusion of the Cogne diorite. The mafic rocks might possibly have an age in the 510–480 Ma range, as measured for the A-type felsic rocks associated to a similar series in Vanoise (loc. Fig. 1, inset) and Val de Rhêmes (Bertrand and Leterrier, 1997; Bertrand et al., 2000a; Guillot et al., 1991) and further North in Valais (Bussy et al., 1996), and their intrusive character would imply a Cambrian or older age for the metasedimentary country-rocks.

### 2.4. Previous data on rock and mineral chemistry

Four major element analyses of the Cogne diorite were found in the literature (I to IV, Table SM1). One analysis by Novarese (1894) was performed on a "schistose rock", interpreted as the result of the "dynamic metamorphosis" of a previously granitic diorite. When compared to the geochemical data available at that time, his analysis allowed him to name the protolith as a quartz diorite, with a primitive plagioclase An<50. Fenoglio and Rigault (1962) gave three analyses, one from a felsic rock comparable to the Novarese analysis (both plotting in the tonalite field of the R1–R2 diagram: Sandrone et al., 2004), and two from more mafic rocks from the Punta Bioula section.

The Cogne diorite host-rocks belong to the Vanoise basement series. Previous analyses of rocks from Vanoise have been used (Beucler et al., 2000; Bussy et al., 1996; Cosma, 1999; Guillot, 1987; Guillot et al., 1993; Saliot, 1978; Leterrier, unpubl. data). They comprise 47 whole-rock data for metashales or metagreywackes, 96 for intercalated mafic rocks and 37 for associated, A-type felsic rocks such as rhyolite and granophyre that, together with the mafic rocks, compose a bimodal magmatic series.

## 3. Petrology and geochemistry

### 3.1. Materials and methods

About 150 polished thin sections were prepared from the samples collected along the Punta Bioula section, and about 50 of them were subjected to micro-chemical investigations using a scanning electron microscope equipped with an energy dispersive system for micro-analysis and elemental mapping (SEM-EDS, Univ. Lille). Dubious mineral phases were also investigated by Raman spectroscopy (green laser 532 nm, model LabRam HR800, Univ. Lille). Fourteen whole-rock analyses (Table 2) were complemented by five Sr–Nd isotope measurements (Table 4). Analyses of major, trace and rare-earth elements were performed at the "Service d'Analyse des Roches et des Minéraux du CRPG-CNRS" at Nancy (in 2004; analytical procedure and precisions: Carignan et al., 2001). $^{143}Nd/^{144}Nd$ and $^{87}Sr/^{86}Sr$ isotope ratios have been determined by Thermal Ionization Mass Spectrometry in five representative samples of the Cogne igneous rocks, following analytical techniques broadly similar to those described by Pin and Santos Zalduegui (1997). The measured ratios are listed in Table 4, along with "initial" values corrected for *in situ* decay of $^{147}Sm$ and $^{87}Rb$ since 360 Ma, by using $^{147}Sm/^{144}Nd$ and $^{87}Rb/^{86}Sr$ ratios calculated from trace element data obtained by ICP-MS.

Views of the fourteen thin sections of the analyzed samples are given as electronic supplementary material (SM2), where their mineral assemblage is also listed (SM3). The sample locations are given in Figs. 1 and 3. Ten samples (1 to 10, Table 2) are representative types from the diorite itself as seen from the field. In order to compare the host rocks to analogous Vanoise rocks (see Section 2.4) and to document potential contamination of the diorite, three host-rocks (11 to 13, Table 2) were analyzed, one black metashale (12) and one metagreywacke (13), which account for a major part of the country-rocks of the Cogne pluton, plus one intercalated mafic rock (11). The last analysis (14) comes from the TPBU (see Section 2.2.2): this massive, fine-grained, albite-rich gneiss with green biotite constitutes the top of the Punta Bioula.

**Table 3**
Selected CIPW-norm data for magmatic rock-types. Analysis numbers refer to the first line of Table 2. CIPW-norms computed using Zhou and Li (2006) Geoplot program. Indicated ranges, in weight %, denote the attribution of Fe, either fully to $Fe^{3+}$ (first value) or fully to $Fe^{2+}$ (second value) — fm, ferro-magnesian minerals — qf, felsic minerals — ox, accessories, including titanite plus rutile (Ttn + Rut) — mg#, 100 × MgO/(MgO + $FeO_{tot}$) — Ap, apatite.

| Analysis | 1 | 2 | 5 | 6 | 7 | 8 | 9 | 10 | 11 |
|---|---|---|---|---|---|---|---|---|---|
| $SiO_2$ wt.% | 62 | 59 | 55 | 53 | 53 | 51 | 51 | 48 | 51 |
| fm | 7–15 | 7–18 | 5–10 | 19–27 | 20–29 | 53–59 | 26–37 | 33–40 | 26–36 |
| qf | 86–83 | 84–80 | 87–85 | 68–65 | 66–63 | 36–35 | 56–52 | 46–46 | 62–62 |
| ox | 6–2 | 9–2 | 8–5 | 13–7 | 14–8 | 11–6 | 18–11 | 21–14 | 12–2 |
| mg# | 55 | 49 | 42 | 62 | 56 | 78 | 61 | 70 | 63 |
| Ttn + Rut | 1.1–0 | 1.6–0 | 0.7–0 | 3.1–0 | 2.7–0 | 1.3–0 | 3.9–0 | 4.6–0 | 1.8–0 |
| Ap | 0.6 | 0.7 | 1.0 | 1.3 | 2.2 | 1.1 | 2.4 | 6.5 | 0.2 |

The range of granitoid rock-types includes all the intermediates between the following end-members (with analysis numbers as in Table 2):

(1) dominant, granodiorite to quartz diorite varieties with feldspar, quartz, amphibole and biotite (1 to 4),
(2) leucocratic, feldspar-rich rock types with biotite, quartz and amphibole (5 to 7),
(3) melanocratic mafic rocks with up to 80% of modal amphibole (8 to 10),
(4) one occurrence of two-mica leucogranite (near Gran Nomenon, Fig. 1; not sampled).

It must be stressed again that the rock classification is tentative. In such a geological context, with added effects of primary complexity, including auto-metamorphic effects, plus the Alpine deformation and HP-metamorphism, any attempt at classifying those metagranitic rocks from modal data inevitably yields poorly assessed names. This adds to the necessity of a geochemical approach.

### 3.2. Rock classification based on geochemical data

#### 3.2.1. Major element and normative data

A selection of CIPW normative data is given in Table 3 for rocks of clearly igneous origin. Their $SiO_2$ contents range from 48 to 62 wt.%. Accordingly, CIPW norms show 1% to 17% of quartz, 35% to 85% of quartz plus feldspar (qf in Table 3), 40% to 7% of ferro-magnesian silicates (fm) and 21% to 4% of oxides and accessories (ox), respectively. From normative data of samples 1 to 7 and following Le Maitre (1976), or from the R1–R2 diagram, the rocks plot as monzonite to granodiorite. Only by allocating a major part of K to biotite, based on its primitive modal content estimated from thin sections (imaged in SM2), these rocks plot into the fields of tonalite, quartz diorite and quartz monzodiorite.

The texturally preserved quartz diorite to granodiorite (anal. 1), which represents the bulk of the pluton to the east of Valsavaranche (Fig. 1), contains approximately equal modal contents of amphibole and pale biotite, totaling around 15 vol.%, their mg# being around 40 from EDS microanalyses. Amphibole and biotite appear to have been significantly modified by the Alpine metamorphism, e.g. partially transformed into chlorite, and Al-in-hornblende barometry proved to be no longer usable. The primitive (Mg-rich?) biotite has been partly transformed into Mg-rich phengite or chlorite, partly into an Al-rich Alpine biotite.

Major element oxide vs. $SiO_2$ plots (Harker's diagrams, not shown) display increasing Al-, Na-, K-contents, and decreasing contents in Ca,

Mg, Fe, Mn, Ti, and P. This may be related to an increasing modal content of alkali feldspar together with a decreasing anorthite component. Major element based classification diagrams do not allow us to give clear-cut rock names, as a probable reflection of either secondary alteration of Alpine age (e.g. samples 3 and 4, more schistose), or primary mineral accumulation processes, especially plagioclase [anal. 5], amphibole [anal. 8 to 10] or both [anal. 6 and 7], and/or apatite [anal. 10] as suggested by petrographic observations. Here, only an AFM plot is shown (Fig. 7a) in order to highlight the contrast between the bimodal pattern, and tholeiitic signature of meta-igneous rocks sampled in the diorite country-rocks, on the one hand, and the continuous array of the diorite data points, in the calc-alkaline field, on the other. The host-rock metapelites plot in the calc-alkaline domain, in correlation with their high albite modal content, in the same field (marked p on diagrams) as the Vanoise metapelite series that was interpreted to derive from probable volcano-sedimentary protoliths (Guillot, 1987; Guillot et al., 1993).

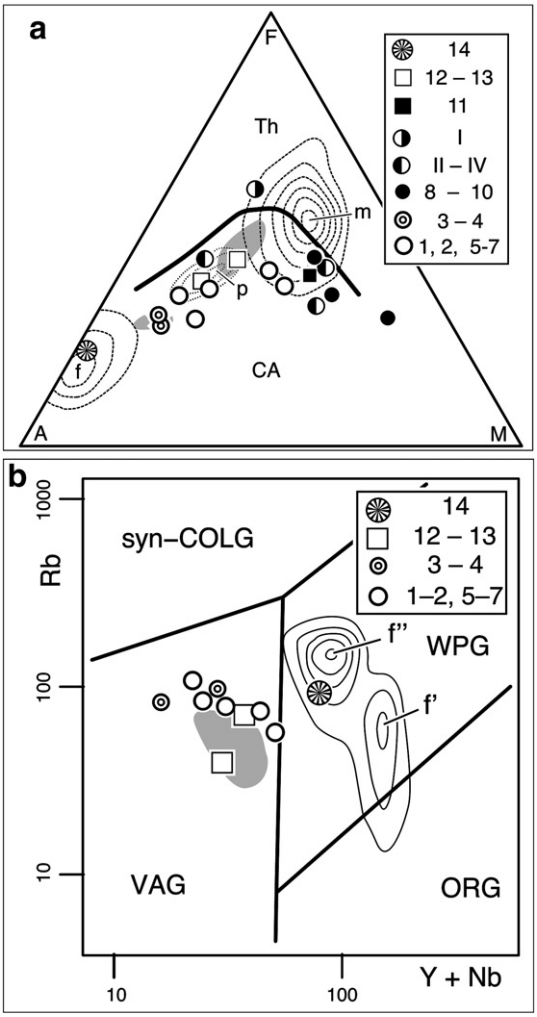


**Fig. 7.** Geotectonic classification diagrams. Numbers I to IV refer to Table SM1, 1 to 14 refer to Table 2; contouring refers to Vanoise basement rocks; gray pattern is for the Limousin tonalites (Shaw et al., 1993). a, AFM triangle (Irvine and Baragar, 1971). Th, domain for tholeiite series — CA, domain for calc-alkaline series — frequency contourings for Vanoise basement analyses refer to (f) 37 Vanoise felsic rocks, (p) 47 Vanoise metapelites, (m) 96 Vanoise mafic rocks — b, Rb vs. Y + Nb diagram (Pearce et al., 1984) — VAG, volcanic arc granites — syn-COLG, syn-collision granites — ORG, oceanic ridge granites — WPG, within-plate granites with contouring for 16 Vanoise felsic rocks: f′, 6 Thyon granite analyses (Bussy et al., 1996) — f″, 10 Mt. Pourri and Val de Rhêmes granophyre analyses (Bertrand et al., 2000a; Beucler et al., 2000; Guillot et al., 1993).

*3.2.2. Trace elements*

In geotectonic classification diagrams based on immobile trace elements, the more felsic diorites (1 to 7) plot in the calc-alkaline field or volcanic arc granitoids (VAG in Fig. 7b; Pearce et al., 1984). More mafic diorites (8 to 10) accordingly plot into the field named "destructive plate margin magmatism" by Wood (1980: Th-Ta-Hf/3 triangle, not shown), where the host-rock tholeiite (11) also plots, though very close to "primitive arc tholeiites". Host-rock metasediments (#12 and 13, with resp. $SiO_2$ contents at 59% and 64%), a family of rocks for which a remote andesite derivation has been suggested based on high $Na_2O/K_2O$ (Guillot et al., 1993), also plot in the VAG field (Fig. 7b). By contrast, in the same diagram the TPBU sample (#14, $SiO_2$ at 72%) plots in the within-plate granitoid field (WPG), as do the felsic rocks from Vanoise.

Chondrite-normalized REE data (Fig. 8a) show steep patterns for both the more felsic diorite types ($La_N/Lu_N$ at 6.7–23.7) and the most mafic varieties ($La_N/Lu_N$ at 8.3–19.1), while porphyritic diorites (Fig. 8a) and host-rock metapelites (Fig. 8b) have a $La_N/Lu_N$ ratio near 7. By contrast, analysis #11, a mafic sample taken from the diorite country-rocks, yields a flat REE-pattern, with a normalized ratio $La_N/Lu_N$ at 1.4 (Fig. 8b) coupled with much lower contents ($\sum$REE of 34 instead of 72 to 491 ppm for the diorite); its REE pattern resembles those observed for mafic rocks from the Vanoise basement (m, after Guillot et al., 1993). A comparison (Fig. 8) of diorite REE patterns with profiles averaged from Vanoise rocks also points to markedly different geochemical styles. Specifically, while the mafic rocks from Vanoise (m or 11, in Fig. 8b) are less REE-rich than their associated

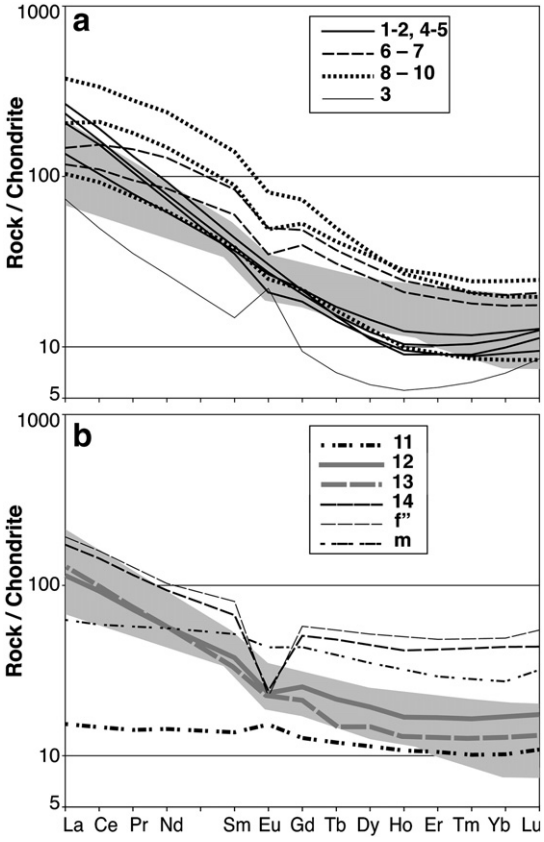


**Fig. 8.** Selected REE-data normalized to chondrite (Sun and McDonough, 1989). a, Cogne diorite rock-types — b, comparison between diorite rock-types (gray zone), country-rocks (11 to 13), TPBU (14), and Vanoise rocks (f″, m). Key to symbols: 1 to 14 refer to analyses listed in Table 2 — f″, m, average of analyses from Vanoise (in litt, cf. Fig. 7) for 5 A-type granophyres, and 2 associated mafic tholeiites, respectively. The gray pattern refers to REE-profiles of Limousin tonalites (Shaw et al., 1993).

felsics (f″), the contrary holds for the Cogne diorite suite. In other words, *mafic diorites are often REE-richer than more felsic diorites* (∑REE at 135–491 ppm, vs. 72–255 ppm, respectively). This reflects the remarkable abundance of titanite, apatite, allanite and zircon in mafic diorites, suggesting a prevailing role of accessory mineral crystallization during the emplacement of the diorite. Invoking hornblende accumulation at the origin of more mafic diorites might also account for their moderate enrichment in HREE relative to felsic types, though our sampling of fresh rock-types (only #8 for mafic rocks) is too limited to allow any definite conclusion.

### 3.3. Information from accessory minerals

A distinctive feature of the various Cogne diorite rock-types is the presence of euhedral, often arrow-shaped titanite crystals up to 1 cm in length. Euhedral titanite was not observed, either in the country-rocks or in the TPBU (anal. 11 to 14), but was preserved even in deformed diorite samples (3–4). In thin section, the rocks also show abundant smaller (0.1 to 0.3 mm), euhedral, zoned allanite crystals, occasionally surrounded by a spongy association of clear epidote and quartz. Zircon is commonly observed as euhedral, concentrically zoned crystals, even in the mafic rock-types. Apatite is also widespread in these rocks, often as euhedral inclusions in the hornblende crystals.

Titanite contains poikilitic, euhedral apatite inclusions, and is often itself included in amphibole. Based on such textural arguments, the proposed order of crystallization is: apatite, Mg-biotite, allanite, titanite, amphibole, plagioclase, Fe-biotite, [garnet-]quartz, K-feldspar. This is somewhat at variance with the canonical Bowen's sequence, and can be attributed to a stepwise crystallization at decreasing depths. Regarding this presumed order of crystallization other arguments have been found considering liquidus and saturation temperatures, as exposed hereafter.

Zircon saturation temperatures of 850 °C were proposed (Guillot et al., 1993) for the Vanoise granophyres (using the approach of Watson and Harrison, 1983) and it is also the temperature obtained here for the TPBU sample (see Section 3.4.3). Results for the diorite rock-types are generally lower, in the range 700–850 °C for the more felsic diorites (1 to 7), and still lower for the most mafic rocks (530–630 °C). Apatite saturation temperatures (Harrison and Watson, 1984) and liquidus temperature (using Sisson and Grove, 1993, or Grove and Juster, 1989, depending on the rock-type, namely mafic types 8 to 10, or more felsic types 1 to 7) were also computed. Modifying a diagram after Harrison and Watson (1984), we propose to use a logarithmic scale for the $P_2O_5$ axis, in order to convert the curves of apatite saturation temperatures into straight lines (Fig. 9; temperatures listed in Table 2). The felsic diorite types (analyses 1 to 7) form an almost linear array, roughly along or slightly above the 900 °C isotherm.

The metaluminous compositions of our samples allow the use of the apatite saturation thermometer, with A/CNK<1 in most analyses (Table 2: except #3 and 4 at 1.02, #5 at 1.04, beside higher values for metasediments #12–13). However, the measured $P_2O_5$ contents might point to some kind of apatite accumulation. This explanation is most straightforward for mafic samples such as analysis #10 with a grossly abnormal 2.78 wt. % of $P_2O_5$, while the representative points of analyses 8 to 10 (Fig. 9) form an almost vertical array [excluding analyses III and IV, as visible outliers: either Fenoglio and Rigault (1962) sampled other rock-types – a tholeiite host-rock, alike analysis 11 that plots nearby? – or phosphorus was not measured accurately in 1962]. Apart from such outliers, it might be considered that the saturation temperature estimates is valid, implying that apatite crystallization, occurred at 900–950 °C. Liquidus temperatures being always higher (in the range 1100 °C–1200 °C) than the latter results suggests they were probably never attained. Taking into account the above-proposed order of crystallization, this interpretation would be in line with progressive crystallization of a deep-originated magma at decreasing depth and temperature, most of this process taking place between 900–950 °C (apatite saturation) and 700–850 °C (zircon saturation).

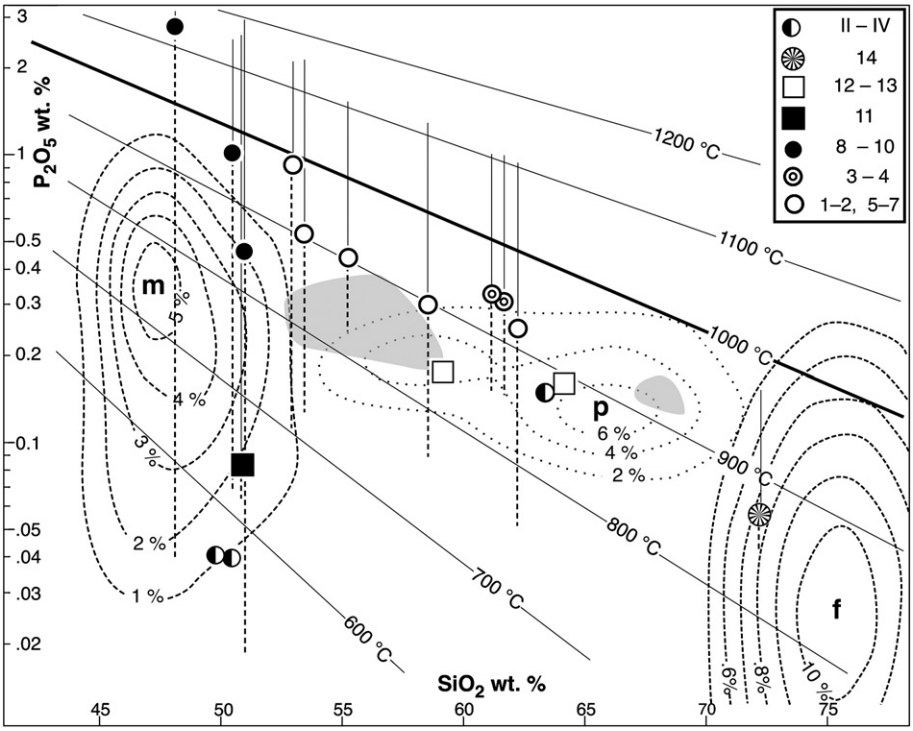


**Fig. 9.** $P_2O_5$ vs. $SiO_2$ with apatite saturation isotherms (after Harrison and Watson, 1984). Key to symbols as in Fig. 7a, sample numbers as in Table SM1 and Table 2. Vertical bars issued upward from each representative points join to the liquidus temperatures around 1100–1150 °C computed from each analysis (Sisson and Grove, 1993); downward dotted bars join to the zircon saturation temperature (Watson and Harrison, 1983).

### 3.4. Peculiar rock-types

#### 3.4.1. Hornblendite

Amphibole-rich rock-types have been reported in the Punta Bioula section (Fenoglio and Rigault, 1959, 1962; Grasso, 1974; Novarese, 1894) and one similar occurrence was mapped (Amstutz, 1962) in the Val de Cogne (Fig. 1). Massive, practically undeformed hornblendites (Fig. 6a,b) occur in apparent continuity with the main pluton SW-wards, on the eastern slope of the Punta Bioula-Punta Bianca ridge (Fig. 3). The relationship of this rock-type with the rest of the pluton has not yet been fully elucidated, since only a handful of small outcrops were tentatively mapped (Fig. 3), though lobate contacts observed between three variously colored diorites (Fig. 6a) suggest that the rocks were concomitantly in a partly molten state. All the previous authors have attributed these amphibole-rich rock-types to local accumulations of mafic minerals. The rocks have a prominent mafic mineral content, with more than 60 vol.%, up to 2 cm in size, dark-green, euhedral amphibole crystals. Whatever the dark color of the rock, quartz is present as interstitial crystals that have kept a magmatic habit and have probably crystallized later than subhedral alkali feldspars. The euhedral amphibole crystals are generally poikilitic (image 8 in suppl. data SM2), with a magnesiohornblende composition in sample #8 (Fig. 6b), while the smaller grains of samples #9 and #10 are actinolite. Apatite, zircon and titanite are idiomorphic and frequently partly included in the magnesiohornblende crystals. The amphiboles of sample #8 also enclose areas of associated Mg-rich phengite and Mg-rich chlorite, from possible phlogopite-rich precursors. The early-formed apatite (see Section 3.3), too, might suggest a deep-seated source to those magmatic rocks, a primitive character being also supported by whole-rock mg# in the range 61–78 (Table 3).

Similar "hollow" amphiboles have been described in appinites (Roach, 1964; Wells and Bishop, 1955), their core enclosing an assemblage of felsic composition, related to a late magmatic episode. The classical appinite occurrences of Great Britain form minor pods distributed marginally relative to the main body of Caledonian granitic plutons, often associated to hypabyssal breccias of the host-rocks. The authors interpreted these rocks as transformed gabbroic relicts in late-magmatic conditions under high water pressure. Accounts from the Canadian Cordillera Westcoast Crystalline Complex (DeBari et al., 1999; Larocque and Canil, 2010) report a continuous range of rock-types from mid-crustal ultramafic cumulates to shallower hornblende gabbro and granodiorite. In a recent reappraisal on the appinite problem (based on outcrops resembling those of Fig. 6a: Pe-Piper et al., 2010), the chemistry of the appinites was shown not to characterize a definite tectonic setting, but rather and only a peculiar magmatic process leading to hydrated mafic rocks. Field evidence of transitional facies between deep-seated mafic cumulates and calc-alkaline, shallower plutons resembling the Cogne diorite, were described in the Western Canadian coastal ranges (DeBari et al., 1999), with a continuous array between hornblende gabbro, hornblendite and hornblende granodiorite.

The Al-in-hornblende barometry [based on a compilation by Tindle and Webb (1994) of the various versions of the Al-in-hornblende barometer], applied to all the EDS-analyzed amphibole crystals, gave consistent results only for cm-sized amphiboles from hornblendite of sample #8, where K-feldspar, biotite and quartz are present as required, yielding $0.35 \pm 0.15$ GPa. Inherited features of higher pressure might be found (1) in the possible phologopite inclusions of those hornblende poikilocrysts, (2) in the presence of apparently early formed epidote streaks inside preserved plagioclase, and (3) in epidote/quartz symplectite around allanite.

#### 3.4.2. Mafic country rocks

In Vanoise, the mafic rocks display a tholeiitic composition. Their tectonic setting was debated, some authors favoring a MORB-character (Guillot, 1987) and others a within-plate, extensional setting (Cosma, 1999). Here one analysis (11 in Table 2) is given for a greenstone septum in metapelites, already mentioned above for its flat REE pattern (Fig. 8b). In thin section, the rock also displays important differences with the diorite mafic rock types, specifically the presence of blue-green Na, Ca-amphibole as a major component, and different accessory minerals: neither allanite, nor idiomorphic apatite nor titanite was observed, and only relictual, tiny shells of zircon could be detected after a careful SEM-examination. Instead, the thin sections are spotted with grains of Fe, Ti-oxide surrounded by leucoxene haloes, suggesting degraded magmatic titanomagnetite, which is characteristic of Vanoise mafic rocks.

#### 3.4.3. TPBU analysis

Based on geochemical data only, marked differences exist between the diorite-hosting unit and the TPBU. The analyzed TPBU rock plots consistently (Figs. 7a, b, 8b, 9) near the field of A-type granophyres from Vanoise. From their geochemistry and field aspect, these "gneiss minuti" [fine-grained] might derive from a rhyolite or ignimbrite protolith. This is in line with other similarities, e.g. the presence of green biotite as the main ferro-magnesian mineral, which was also observed in Vanoise granophyres, themselves of hypabyssal character (Beucler et al., 2000), together with very low mg# and Ca, Mg-contents.

## 4. Igneous sources

### 4.1. Bulk composition melts

Not excluding *a priori* a mantle origin, identifying the type of a possible crustal source for the diorite can be attempted through a major element diagram (Fig. 10a) devised from a compilation of experimental melt analyses (Altherr et al., 2000). Among the nearby rocks, only the TPBU metavolcanite (anal. 14) plots alike melts from metagreywackes. The host-rock metapelites (anal. 12–13) plot inside the domain of Vanoise metapelites (denoted by "p" contouring in Fig. 10a), and the mafic level from country-rocks (anal. 11) into the domain of Vanoise mafics ("m" contouring), both out of crustal melt fields. The Vanoise granophyres and granites ("f") plot clearly apart from the diorite, in the field of melts from metapelites. While the hornblendite samples (8–10) have an ambiguous position, out of all the experimental fields for crustal melts, the dominant felsic rock-types of the Cogne diorite (anal. 1–7) plot into the field of partial melts issued from metabasaltic to metatonalitic sources.

### 4.2. Sr–Nd radiogenic isotopes

Five diorite, two more felsic rock-types (1, 4), one intermediate rock (5) and two hornblendites (8, 9) have been measured (Table 4). The age-corrected Nd isotope data, expressed with the usual epsilon-notation, display a limited range of values, from $-1.2$ to $+0.9$, as do $^{87}Sr/^{86}Sr_{360}$, from 0.7054 (a mafic rock) to 0.7063 (the most $SiO_2$-rich rock).

In spite of a relatively large spread of $^{147}Sm/^{144}Nd$ (from 0.0928 to 0.1215), no clear correlation can be observed with $\varepsilon Nd_{360}$ values, in contrast with what would occur if combined assimilation and fractional crystallization (AFC) had played an important role during the late-stage evolution of the magmas which formed the Cogne intrusive body. Likewise, there is no inverse relationship between $\varepsilon Nd_{360}$ values and $^{87}Sr/^{86}Sr_{360}$ ratios, at variance with what is commonly found in igneous systems. Admittedly, age-corrected $^{87}Sr/^{86}Sr$ isotopes do not provide very robust information due to the possibly very significant mobility of both Rb and Sr during deformation and metamorphism, although the relatively small spread of initial ratios may suggest that gross disturbances did not play a major role in this case. If not disturbed at a post-igneous stage, the more radiogenic Sr isotope signature observed in the most silica-rich rock might be interpreted to reflect the assimilation of hydrous fluids relatively rich in $^{87}Sr$, but unable to induce

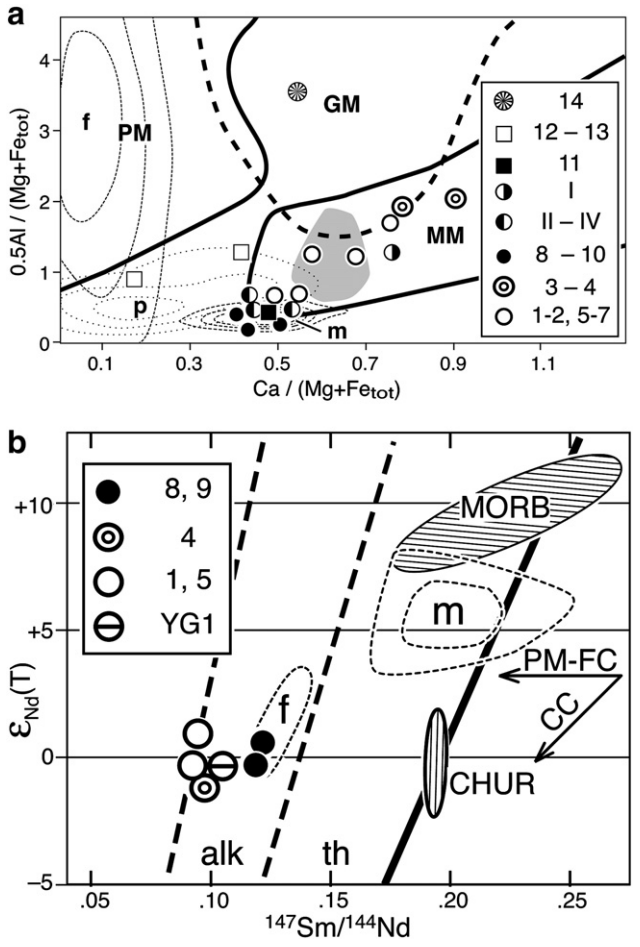


**Fig. 10.** Magmatic source diagrams. Key to sample numbers as in Table SM1 and Table 2, plus: YG1, unspecified Cogne diorite sample from Cosma (1999). a, Diagram A/MF vs. C/MF (from a compilation by Altherr et al., 2000) with Vanoise basement contourings (m, p, f) as in Fig. 9. — MM, partial melts from metabasaltic to metatonalitic sources — GM, partial melts from metagreywackes — PM, partial melts from metapelitic sources. b, $\varepsilon_{Nd}(T)$ vs. $^{147}Sm/^{144}Nd$ after DePaolo (1988) — PM-FC, partial melt-fractional crystallization vector — CC, crustal contamination vector — m, f: contouring of the Vanoise magmatic rocks, after Cosma (1999) using, respectively, 8 mafic rocks and 3 felsic rocks.

any shift of Nd isotope composition due to their typically REE-poor characteristics.

Albeit of little (if any) geological significance due to the most likely multi-stage evolution of the source reservoir(s) of the *ca.* 360 Ma magmas, $T_{DM}$ model ages (DePaolo, 1981) are rather tightly grouped, and much older (0.78–0.98 Ga) than the igneous emplacement age established by U–Pb zircon dating. This suggests that, if an ultimate depleted mantle source reservoir was tapped, ancient recycled materials were also involved.

Taken at face value, the $\varepsilon Nd_{360}$ data close to the chondritic (or Bulk Silicate Earth) value indicate that the overall, average source materials of the Cogne diorite magma were, on a time-integrated basis, neither enriched, nor depleted in Sm relative to Nd. Whatever its possible geological interpretation, this feature is shared by many continental flood basalts worldwide. In practical terms, this might reflect a direct derivation from a source reservoir with $\varepsilon Nd_{360} \sim 0$, which might have been extracted, for example, from a typical, long-term depleted mantle (with radiogenic – i.e., positive εNd – isotope signature) in the Late Proterozoic, as inferred from $T_{DM}$ model ages. Another possible scenario would envision a long-term depleted mantle source which suffered contamination by old crustal materials (enriched in LREE and with negative εNd) recycled into the upper mantle via subduction, at some undefined time prior to 360 Ma.

Alternatively, the Nd isotope signature of the Cogne magmas might reflect primary mafic melts extracted from a depleted (with $\varepsilon Nd_{360} > 0$) mantle source, that were contaminated by assimilation of materials with negative $\varepsilon Nd_{360}$ during their ascent through, and possible ponding in, the continental crust. In this interpretation, the major assimilation would have been accompanied, or followed, by a process of homogenization of the blended magmas before final ascent to their emplacement level, thereby accounting for their broadly homogeneous Nd and Sr whole-rock isotopic features.

Our isotopic data set is too limited, by itself, to allow us to favor any of these possible interpretations.

For the sake of completeness, the Cogne diorite characters have to be confronted to data from the Vanoise basement, to which belonged the present country-rocks. Cosma (1999) performed one Sm–Nd isotopic analysis of the Cogne diorite (his sample YG1) in agreement with our results (0.1039, 0.512422 and −0.7 for $^{147}Sm/^{144}Nd$, $^{143}Nd/^{144}Nd$ and $\varepsilon Nd_{300\ Ma}$, resp.), hence allowing comparisons. Most of his analyses concern Vanoise mafic and felsic rocks. Adding his data to a plot of $\varepsilon Nd_i$ vs. $^{147}Sm/^{144}Nd$ (Fig. 10b), the vectors MORB-to-diorite and Vanoise-mafics-to-diorite almost parallel the crustal contamination vector (CC, after DePaolo, 1988). However, an ancient MORB as source would yield magmas with highly radiogenic Nd, which was not observed in the present case.

**Table 4**
Isotope data. Sample numbers refer to the first line of Table 2.

| Sample | 1 | 4 | 5 | 8 | 9 |
|---|---|---|---|---|---|
| Sm | 5.27 | 5.80 | 6.65 | 5.77 | 13.3 |
| Nd | 33.6 | 36.0 | 43.3 | 28.7 | 67.8 |
| $^{147}Sm/^{144}Nd$ | 0.0948 | 0.0974 | 0.0928 | 0.1215 | 0.1186 |
| $^{143}Nd/^{144}Nd$ | 0.512444 | 0.512345 | 0.512381 | 0.512490 | 0.512439 |
| ±2 S.E. | 0.000004 | 0.000004 | 0.000008 | 0.000005 | 0.000019 |
| $\varepsilon Nd_{360Ma}$ | 0.9 | −1.2 | −0.3 | 0.5 | −0.3 |
| $T_{DM}$ (Ga) | 0.78 | 0.92 | 0.84 | 0.97 | 0.98 |
| Rb | 108 | 89.5 | 85.7 | 21.7 | 54.9 |
| Sr | 581 | 876 | 1052 | 232 | 319 |
| $^{87}Rb/^{86}Sr$ | 0.538 | 0.296 | 0.236 | 0.271 | 0.498 |
| $^{87}Sr/^{86}Sr$ | 0.709082 | 0.707539 | 0.707083 | 0.706768 | 0.708130 |
| +/−2 S.E. | 0.000006 | 0.000004 | 0.000005 | 0.000004 | 0.000004 |
| $^{87}Sr/^{86}Sr_{360Ma}$ | 0.7063 | 0.7060 | 0.7059 | 0.7054 | 0.7056 |

## 5. Discussion and conclusions

### 5.1. I-type characters for the Cogne diorite

Based on a wealth of criteria, an I-type may be proposed for the Cogne diorite: a magmatic assemblage with amphibole, pale biotite, titanite, allanite ± epidote; no monazite and no muscovite; $0.7054 < {}^{87}Sr/^{86}Sr_{360} < 0.7063$, $-1.2 < \varepsilon Nd_{360} < +0.9$ (Barbarin, 1999; Clemens et al., 2011; McCulloch and Chappell, 1982). For comparison purposes, the I-type quartz-diorites of Limousin (Shaw et al., 1993) were plotted in the various diagrams (Figs. 7 to 10). With $SiO_2$-contents at 53–58% for seven plutons, plus one at 68%, an age range at 350–380 Ma, and their isotopic values $0.7047 < {}^{87}Sr/^{86}Sr_i < 0.7059$, $-0.7 < \varepsilon Nd_{360} < +1.8$, the Limousin quartz diorites are directly comparable to the Cogne diorite. They have been considered as related to a N-directed subduction by some authors (Refs. in Shaw et al., 1993). Further investigations, based on a larger number of Late Devonian–Early Carboniferous plutons in the northern part of French Massif central, favored a pre-collisional, S-ward subduction of the Rheic oceanic crust (Pin and Paquette, 2002) as the cause of this magmatism.

A number of uncertainties prevent any definite correlation between Internal Penninic basement units and possible counterparts of the stable (during Alpine times) European plate. The pre-Alpine

location of the Cogne diorite-bearing unit may have been somewhere to the South of Marseille during the Early Mesozoic times after Stampfli and Kozur (2006), and earlier motions, e.g. along major strike-slip faults of Carboniferous age, may have brought our unit from unpredictable distances and directions. Following the same authors, at 360 Ma the Vanoise, as part of the Briançonnais terrane, belonged to a narrow continental (?) ribbon between two opposed subducting oceanic crusts, the S-directed subduction of Rheno-Hercynian oceanic crust, to the North, and the N-directed subduction of Paleotethys oceanic crust, to the South (Stampfli and Kozur, 2006: their Fig. 1C); this continental ribbon would have been previously separated at ~400 Ma from the N margin of Gondwana by the Paleotethyan rifting (ibid., Fig. 1A–B). Hence, a possible similarity exists with the above cited scenario of Pin and Paquette (2002). Nevertheless, the "destructive plate margin" characters of the Cogne diorite documented in the present paper may at least contribute to a better knowledge of this important igneous marker of paleogeodynamic settings.

### 5.2. Emplacement conditions

Our geochemical data, which are probably quite comparable for most I-type rocks, yield: liquidus temperatures tending toward 1200 °C for hornblendites (from major element contents; Grove and Juster, 1989), and near 1100 °C for more felsic diorites; apatite saturation temperatures at 950–900 °C (based only on felsic rocks); zircon saturation temperatures at 700–850 °C for the ordinary felsic diorites and at 630–530 °C for the hornblendites. Pressures from Al-in-hornblende barometry on the latter rocks can be estimated at $0.35 \pm 0.15$ GPa (i.e. 6 to 15 km in depth) for final emplacement, while phlogopite-related inclusions of the same hornblende crystals suggest a protracted history of crystallization at decreasing depths and temperatures. Other P–T criteria, out of the scope of this paper, are being searched in the mineralogy of the proximal hornfelses, which are rich in pre-Alpine, pea-sized garnets (work in progress).

### 5.3. Alpine context

A major shear zone exists at the top of the diorite, possibly some hundreds of meters thick when taking into account the recumbent folds of the TPBU. It dips to the W, and might be equivalent to the Feleumaz shear zone, a W-dipping imbricate of basement, cover and ophiolitic rocks, that Malusà et al. (2005) have described nearby, along the western flank of Val de Rhêmes (loc. Fig. 1). This shear zone comprises a Vanoise-type granophyre dated at $511 \pm 9$ Ma (Bertrand et al., 2000a). This is in line with many similarities documented above between our A-type TPBU sample and the Vanoise felsic rocks, and would suggest an Early Paleozoic age for the TPBU protoliths. Following Malusà et al. (2005), the TPBU might represent an Alpine mélange. From this respect it would be interesting to investigate the nature and age of the associated augengneiss. Whatever the answers and waiting for further field work, instead of the classical tectonic model of a two-limbed "pli en retour du Valsavaranche", we have evidenced here a highly dissymmetric structure in the Punta Bioula massif, with the diorite almost undeformed at the footwall of the highly deformed TPBU sheet.

### 5.4. Established facts and future research

The analyses of host-rocks in the present study confirm that they belong to the Vanoise series. The host-rocks have the same characters as typical Vanoise rocks, a fact that adds a nail in the coffin of the traditional attribution to Permo-Carboniferous of all the Penninic basement protoliths. Field occurrences of flattened sill-and-dyke systems suggest that the tholeiitic mafic levels of this basement were intrusive in the metapelite–metagreywacke series, which might be of Cambrian or even older age.

Neither the country-rock metapelites, nor other Lower Paleozoic basement units like the Ruitor massif (Guillot et al., 2002), the latter as possible candidate for an ~360 Ma lower crust, have yet been investigated isotopically. Obviously, further data are needed before reconstituting the local lithosphere at 360 Ma.

Supplementary data to this article can be found online at http://dx.doi.org/10.1016/j.lithos.2012.04.010.

## Acknowledgments

Jean-Luc Potdevin, Marie Lefranc and Monique Gentric (UMR 8110 PBDS-CNRS) helped in funding the analyses. The staff and director of the Parco Nazionale del Gran Paradiso have allowed sampling inside the Park and sheltered us in mountain refuges of Orvieille and Gran Nomenon. Renaud Caby (Montpellier) and Enzo Callegari (Torino) provided unpublished documentation, and Marco Malusà (Milano) proposed new ideas on the Alpine shear zones. Abdoulaye Baldé, Thomas Maurin, Bénédicte Knafel, Riccardo Polino, Floriane van Leendert and Frédérique Liotard-Schneider took part to the field and lab work. We also thank Y. Rolland and an anonymous reviewer for their constructive comments. We miss Jean-Michel Bertrand, still on the Punta Bioula in September, 2009, who passed away on March 18th, 2011.

## References

Altherr, R., Holl, A., Hegner, E., Langer, C., Kreuzer, H., 2000. High-potassium, calc-alkaline I-type plutonism in the European Variscides: northern Vosges (France) and northern Schwarzwald (Germany). Lithos 50, 51–73.
Amstutz, A., 1962. Notice pour une carte géologique de la vallée de Cogne et de quelques autres espaces au sud d'Aoste. Archives des Sciences, Société de Physique et d'Histoire Naturelle de Genève (eds) 15, 1–104.
Angiboust, S., Agard, P., Jolivet, L., Beyssac, O., 2009. The Zermatt-Saas ophiolite: the largest (60-km wide) and deepest (c. 70–80 km) continuous slice of oceanic lithosphere detached from a subduction zone? Terra Nova 21, 171–180.
Argand, E., 1910. Les nappes de recouvrement des Alpes Pennines et leurs prolongements structuraux, une carte tectonique et deux stéréogrammes avec texte explicatif. Beiträge zur Geologischen Karte der Schweiz, n.F. XXXI 25 pp..
Argand, E., 1911. Sur les plissements en retour et la structure en éventail dans les Alpes occidentales (17 mai 1911). Bulletin de la Société Vaudoise des Sciences Naturelles XLVII, XXXIII–XXXVI.
Barbarin, B., 1999. A review of the relationships between granitoid types, their origins and their geodynamic environments. Lithos 46, 605–626.
Beltrando, M., Lister, G.S., Forster, M., Dunlap, W.J., Fraser, G., Hermann, J., 2009. Dating microstructures by the 40Ar/39Ar step-heating technique: deformation–pressure–temperature–time history of the Penninic Units of the Western Alps. Lithos 113, 801–819.
Bertrand, J.-M., Leterrier, J., 1997. Granitoïdes d'âge Paléozoïque inférieur dans le socle de Vanoise méridionale: géochronologie U–Pb du métagranite de l'Arpont (Alpes de Savoie, France). Comptes Rendus de l'Académie des Sciences – Série IIa 325, 839–844.
Bertrand, J.-M., Guillot, F., Leterrier, J., 2000a. Early Paleozoic U–Pb age of zircons from metagranophyres of the Grand-Saint-Bernard Nappe (zona interna, Aosta Valley, Italy) [abridged English version]. Comptes Rendus de l'Académie des Sciences – Série IIa 330, 473–478.
Bertrand, J.-M., Pidgeon, R.T., Leterrier, J., Guillot, F., Gasquet, D., Gattiglio, M., 2000b. SHRIMP and IDTIMS U–Pb zircon ages of the pre-Alpine basement in the Internal Western Alps (Savoy and Piemont). Schweizerische Mineralogische und Petrographische Mitteilungen 80, 225–248.
Bertrand, J.-M., Paquette, J.-L., Guillot, F., 2005. Permian zircon U–Pb ages in the Gran Paradiso massif: revisiting post-Variscan events in the Western Alps. Schweizerische Mineralogische und Petrographische Mitteilungen 85, 15–29.
Beucler, M., Guillot, F., Hernandez, J., 2000. Granophyric rocks of the Mont Pourri area (northern Vanoise, Savoie, France): lithostratigraphy and petrology. Bulletin de la Société Vaudoise de Sciences Naturelles 87, 29–60.
Bousquet, R., 2008. Metamorphic heterogeneities within a single HP unit: overprint effect or metamorphic mix? Lithos 103, 46–69.
Bucher, S., Bousquet, R., 2007. Metamorphic evolution of the Briançonnais units along the ECORS-CROP profile (Western Alps): new data on metasedimentary rocks. Swiss Journal of Geosciences 100, 227–242.
Bussy, F., Derron, M.-H., Jacquod, J., Sartori, M., Thélin, P., 1996. The 500 Ma-old Thyon metagranite: a new A-type granite occurrence in the western Penninic Alps (Wallis, Switzerland). European Journal of Mineralogy 8, 565–575.
Caby, R., 1968. Contribution à l'étude structurale des Alpes Occidentales: subdivisions stratigraphiques et structure de la zone du Grand-Saint-Bernard dans la partie

sud du Val d'Aoste (Italie). Travaux du Laboratoire de Géologie de la Faculté des Sciences de Grenoble 44, 95–111.
Carignan, J., Hild, P., Mevelle, G., Morel, J., Yeghicheyan, D., 2001. Routine analyses of trace elements in geological samples using flow injection and low pressure on-line liquid chromatography coupled to ICP-MS: a study of geochemical reference materials BR, DR-N, UB-N, AN-G and GH. Geostandards Newsletter: The Journal of Geostandards and Geoanalysis 25, 187–198.
Cigolini, C., 1992. Note illustrative alla carta geologica del ricoprimento del Gran San Bernardo tra la Valsavarenche e la Val di Rhêmes (Valle d'Aosta) scala 1:20.000. Documento tecnico, Regione Autonoma della Valle d'Aosta - Assessorato Agricoltura, Forestazione e Risorse Naturali (eds.), 25 p.
Cigolini, C., 1995. Geology of the Internal Zone of the Grand Saint Bernard Nappe: a metamorphic Late Paleozoic volcano-sedimentary sequence in South-Western Aosta Valley (Western Alps). In: Lombardo, B. (Ed.), Studies on Metamorphic Rocks and Minerals of the Western Alps. A Volume in Memory of Ugo Pognante, 13. Bollettino del Museo Regionale di Scienze Naturali, Torino, pp. 293–328.
Clemens, J.D., Stevens, G., Farina, F., 2011. The enigmatic sources of I-type granites: the peritectic connexion. Lithos 126, 174–181.
Cosma, L., 1999. Géologie et magmatisme paléozoïque en Vanoise septentrionale (La Sauvire, Plan Richard). Implications géodynamiques. Unpubl. mem., Dipl. Géol. Min. Univ. Lausanne, 117 p.
DeBari, S.M., Anderson, R.G., Mortensen, J.K., 1999. Correlation among lower to upper crustal components in an island arc: the Jurassic Bonanza arc, Vancouver Island, Canada. Canadian Journal of Earth Sciences 36, 1371–1413.
Debelmas, J., Caby, R., Desmons, J., Dabrovsky, H., Fabre, J., Mercier, D., Pachoud, A., 1991. Notice explicative de la Feuille Sainte-Foy-Tarentaise. Carte géol. Fr. (1/50 000), Bureau de Recherches Géologiques et Minières eds, Orléans 728, 43 p.
DePaolo, D.J., 1981. Neodymium isotopes in the Colorado Front Range and crust–mantle evolution in the Proterozoic. Nature 291, 193–196.
DePaolo, D.J., 1988. Neodymium isotope geochemistry: an introduction. Minerals and rocks Series, Springer eds. Berlin-New York 20, XI-187 p.
Fenoglio, M., Rigault, G., 1959. Studi geologico-petrografici sulla formazione dioritica di Cogne - Valsavaranche (Valle d'Aosta). Rendiconti della Accademia nazionale dei Lincei VIII (XXVI), 335–344.
Fenoglio, M., Rigault, G., 1962. Studi geologico-petrografici sulla formazione dioritica di Cogne - Valsavaranche: gabbrodiorite della zona Punta Bioula - Punta Bianca (Valle d'Aosta). Atti della Accademia delle Scienze di Torino 96, 506–516.
Gabudianu Radulescu, I., Rubatto, D., Gregory, C., Compagnoni, R., 2009. The age of HP metamorphism in the Gran Paradiso Massif, Western Alps: a petrological and geochronological study of "silvery micaschists". Lithos 110, 95–108.
Grasso, E., 1974. Studi geologico-petrografici sul massiccio intrusive di Cogne-Valsavaranche, con particolare riguardo ai suoi contatti. Unpubl. Thesis Mem. Ist. Petr. Univ. Torino., 219 p.
Grove, T.L., Juster, T.C., 1989. Experimental investigations of low-Ca pyroxene stability and olivine-pyroxene-liquid equilibria at 1-atm in natural basaltic and andesitic liquids. Contributions to Mineralogy and Petrology 103, 287–305.
Guillot, F., 1987. Géologie de l'Antépermien de Vanoise septentrionale (zone briançonnaise interne, Alpes occidentales, Savoie, France). Unpubl. mem., Thèse Doct. Univ. Lille, 280 p.
Guillot, F., 2011. Syn-emplacement softening of host-rock around the Cogne diorite pluton (W-Alps, Valle d'Aosta). VII Hutton Symposium, Avilà 4–9 July 2011, pp. 63–64. Abstract volume.
Guillot, F., Liégeois, J.-P., Fabre, J., 1991. Late Cambrian Mt Pourri granophyres, first dating by U–Pb on zircon of a basement in the internal French Alps (Penninic Alps, Briançonnaise Zone, Vanoise) [abridged English version]. Comptes Rendus de l'Académie des Sciences – Série II 313, 239–244.
Guillot, F., Desmons, J., Ploquin, A., 1993. Lithostratigraphy and geochemical composition of the Mt. Pourri volcanic basement, Middle Penninic W-Alpine zone, France. Schweizerische Mineralogische und Petrographische Mitteilungen 73, 319–334.
Guillot, F., Schaltegger, U., Bertrand, J.M., Deloule, É., Baudin, T., 2002. Zircon U–Pb geochronology of Ordovician magmatism in the polycyclic Ruitor Massif (Internal W-Alps). International Journal of Earth Sciences 91, 964–978.
Harrison, T.M., Watson, E.B., 1984. The behavior of apatite during crustal anatexis: equilibrium and kinetic considerations. Geochimica et Cosmochimica Acta 48, 1467–1477.
Hermann, F., 1925. Sur le faisceau de plis en retour de Valsavarenche et les prolongements de l'éventail de Bagnes dans les Alpes franco-italiennes. Comptes Rendus de l'Académie des Sciences 180, 1515–1517.
Irvine, T.N., Baragar, W.R.A., 1971. A guide to the chemical classification of the common volcanic rocks. Canadian Journal of Earth Sciences 8, 523–548.
Larocque, J., Canil, D., 2010. The role of amphibole in the evolution of arc magmas and crust: the case from the Jurassic Bonanza arc section, Vancouver Island, Canada. Contributions to Mineralogy and Petrology 159, 475–492.
Le Maitre, R.W., 1976. Some problems of the projection of chemical data into mineralogical classifications. Contributions to Mineralogy and Petrology 56, 181–189.
Malusà, M.G., Polino, R., Martin, S., 2005. The Gran San Bernardo nappe in the Aosta valley (western Alps): a composite stack of distinct continental crust units. Bulletin de la Société Géologique de France 176, 417–431.
McCulloch, M.T., Chappell, B.W., 1982. Nd isotopic characteristics of S- and I-type granites. Earth and Planetary Science Letters 58, 51–64.
Michard, A., Goffé, B., 2005. Recent advances in Alpine studies: tracking the Caledonian–Variscan belt in the internal western Alps. Comptes Rendus Geoscience 337, 715–718.
Novarese, V., 1894. Dioriti granitoidi e gneissiche della Valsavaranche (Alpi Graie). Bolletino del Reale Comitato Geologico d'Italia 3, 275–301.
Novarese, V., 1909. Il profilo della Grivola (Alpi Graie). Bolletino del Reale Comitato Geologico d'Italia 40, 497–525.
Pearce, J.A., Harris, N.B.W., Tindle, A.G., 1984. Trace element discrimination diagrams for the tectonic interpretation of granitic rocks. Journal of Petrology 25, 956–983.
Pe-Piper, G., Piper, D.J.W., Tsikouras, B., 2010. The late Neoproterozoic Frog Lake hornblende gabbro pluton, Avalon Terrane of Nova Scotia: evidence for the origins of appinites. Canadian Journal of Earth Sciences 47, 103–120.
Pin, C., Paquette, J.-L., 2002. Sr–Nd isotope and trace element evidence for a Late Devonian active margin in northern Massif-Central (France). Geodinamica Acta 15, 63–77.
Pin, C., Santos Zalduegui, J.F., 1997. Sequential separation of light rare-earth elements, thorium and uranium by miniaturized extraction chromatography: application to isotopic analyses of silicate rocks. Analytica Chimica Acta 339, 79–89.
Ring, U., Collins, A.S., Kassem, O.K., 2005. U–Pb SHRIMP data on the crystallization age of the Gran Paradiso augengneiss, Italian Western Alps: further evidence for Permian magmatic activity in the Alps during break-up of Pangea. Eclogae Geologicae Helvetiae 98, 363–370.
Roach, R.A., 1964. Mineral banding and appinites in the Bon Repos meladiorite, Guernsey, Channel Islands. Proceedings of the Geologists' Association 75, 185–198.
Saliot, P., 1978. Le métamorphisme dans les Alpes françaises. Unpubl. mem., Thèse Univ. Paris-Orsay, 190 p.
Sandrone, R., Colombo, A., Fiora, L., Fornaro, M., Lovera, E., Tunesi, A., Cavallo, A., 2004. Contemporary natural stones from the Italian western Alps (Piedmont and Aosta Valley Regions). Periodico di Mineralogia 73, 211–226.
Shaw, A., Downes, H., Thirlwall, M.F., 1993. The quartz-diorites of Limousin: elemental and isotopic evidence for Devono-Carboniferous subduction in the Hercynian belt of the French Massif Central. Chemical Geology 107, 1–18.
Sisson, T.W., Grove, T.L., 1993. Temperatures and H2O contents of low-MgO high-alumina basalts. Contributions to Mineralogy and Petrology 113, 167–184.
Stampfli, G.M., Kozur, H.W., 2006. Europe from the Variscan to the Alpine cycles. Geological Society, London, Memoirs 32, 57–82.
Sun, S.-s., McDonough, W.F., 1989. Chemical and isotopic systematics of oceanic basalts: implications for mantle composition and processes. Geological Society of London. Special Publications 42, 313–345.
Tindle, A.G., Webb, P.C., 1994. Probe-AMPH—A spreadsheet program to classify microprobe-derived amphibole analyses. Computers & Geosciences 20, 1201–1228.
Watson, E.B., Harrison, T.M., 1983. Zircon saturation revisited: temperature and composition effects in a variety of custal magma types. Earth and Planetary Science Letters 64, 295–304.
Wells, A.K., Bishop, A.C., 1955. An appinitic facies associated with certain granites in Jersey, Channel Islands. Quarterly Journal of the Geological Society 111, 143–166.
White, D.A., Roeder, D.H., Nelson, T.H., Crowell, J.C., 1970. Subduction. Geological Society of America Bulletin 81, 3431–3432.
Wood, D.A., 1980. The application of a Th–Hf–Ta diagram to problems of tectonomagmatic classification and to establishing the nature of crustal contamination of basaltic lavas of the British Tertiary Volcanic Province. Earth and Planetary Science Letters 50, 11–30.
Zhou, J., Li, X., 2006. GeoPlot: an Excel VBA program for geochemical data plotting. Computers & Geosciences 32, 554–560.